A Preliminary Investigation of Whether High Resolution Cervical Auscultation Signals Present Variations Between Thin Liquid Barium and Water Swallows

by

Ryan Schwartz

B.S. in Electrical Engineering, University of Pittsburgh, 2017

Submitted to the Graduate Faculty of

the Swanson School of Engineering in partial fulfillment

of the requirements for the degree of

Master of Sciences

University of Pittsburgh

2021

UNIVERSITY OF PITTSBURGH

SWANSON SCHOOL OF ENGINEERING

This thesis was presented

by

Ryan Schwartz

It was defended on

May 28th 2021

and approved by

Ervin Sejdić Ph.D.

Associate Professor, Department of Electrical and Computer Engineering

Murat Akcakaya, Ph.D.

Associate Professor, Department of Electrical and Computer Engineering

Ahmed Dallal, Ph.D.

Assistant Professor, Department of Electrical and Computer Engineering

James Coyle, Ph.D.

Department of Communication Science and Disorders

A Preliminary Investigation of Whether High Resolution Cervical Auscultation Signals Present Variations Between Thin Liquid Barium and Water Swallows

Ryan Schwartz, M.S.

University of Pittsburgh, 2021

Dysphagia, commonly referred to as abnormal swallowing, affects millions of people annually. If not diagnosed expeditiously, dysphagia can lead to more severe complications, such as pneumonia, nutritional deficiency, and dehydration. Bedside screening is the first step of dysphagia characterization and is usually based on pass/fail tests in which a nurse observes the patient performing water swallows to look for overt signs of dysphagia such as coughing. Though quick and convenient, bedside screening provides low-level judgment of impairment, lacks standardization, and suffers from subjectivity. Recently, high resolution cervical auscultation (HRCA) has been investigated as a less expensive and non-invasive method to diagnose dysphagia. It has shown strong preliminary evidence of its effectiveness in penetration-aspiration detection as well as multiple swallow kinematics. HRCA signals have been investigated in conjunction with videofluoroscopy exams performed using barium boluses. An HRCA-based bedside screening is highly desirable to expedite initial dysphagia diagnosis and overcome all drawbacks of current pass/fail screening tests. However, all research conducted using HRCA in dysphagia is based on thin liquid barium boluses and thus not guaranteed to provide valid results for water boluses. If HRCA signals show no significant differences between water and thin liquid barium boluses, then the same algorithms developed from thin liquid barium can be directly applied with water. This study investigates the similarities and differences between HRCA signals from thin liquid barium swallows and water swallows. Multiple features from the time, frequency, time-frequency, and information-theoretic domain were extracted from each type of swallow, and a group of linear mixed models was tested to determine the significance of differences. Machine learning classifiers were fit to the data as well to determine if the swallowed material (thin liquid barium or water) can be correctly predicted from an unlabeled set of HRCA signals. The results demonstrated no systematic difference between the HRCA signals of thin liquid

barium swallows and water swallows. While no systematic difference exists, the evidence of complete conformity between HRCA signals of both materials was inconclusive. These results must be validated further to demonstrate similarity between the HRCA signals of thin liquid barium swallows and water swallows.

Keywords: High Resolution Cervical Auscultation, Dysphagia, Bedside Screening, Thin Liquid Barium, Water.

Table of Contents

List of Tables

List of Figures

Preface

I would like to thank my advisor, Dr. Ervin Sejdić, for his guidance, support, and encouragement. I would like to thank Subashan Perera for his help in this study and James Coyle for his expertise in the subject. I would like to thank my colleagues, Yassin Khalifa and Erin Lucatorto, for their support, advice, and patience in this study and laboratory work. Lastly, I am grateful for the support of my family and friends throughout this process. Without the help of all involved, this thesis would not have been possible.

1.0 Introduction

1.1 Motivation for This Research

Dysphagia, also known as abnormal swallowing, is a term which indicates swallowing difficulties. The term derives from the Greek term 'dys' meaning 'disordered' or 'ill,' and 'phago' meaning 'eat' or 'swallow.' Dysphagia is categorized as swallowing dysfunction that occurs between the oral cavity and the stomach [1]. Dysphagia can be categorized into two sections: esophageal dysphagia and oropharyngeal dysphagia. Esophageal dysphagia is related to difficulty transporting a bolus through the esophagus, while oropharyngeal dysphagia is related to swallowing difficulties within the oral cavity and pharynx [2].

1.1.1 Esophageal Dysphagia

Esophageal dysphagia normally results from mechanical or muscular dysfunction. A typical mechanical cause is esophageal rings and webs, and typical neuromuscular causes include achalasia and scleroderma. A patient with esophageal dysphagia will typically describe the feeling of food 'sticking' behind the sternum. Esophageal dysphagia often manifests in the pharynx. The symptoms for esophageal dysphagia include regurgitation, gastroesophageal reflux disease, and weight loss [1].

For a patient suspected to have esophageal dysphagia, an evaluation can include a standard barium swallow or upper gastrointestinal endoscopy. An upper gastrointestinal endoscopy is usually required for the confirmation of esophageal dysphagia. Many clinicians utilize gastrointestinal endoscopy for the initial diagnostic evaluation of esophageal dysphagia. These tests account for 20% of all upper gastrointestinal endoscopes in the United States [3, 4]. Other diagnostic tests to confirm a diagnosis are available, such as high-resolution esophageal manometry. If required, these techniques are normally utilized after the initial diagnostic of a barium swallow or upper gastrointestinal endoscopy [5].

1.1.2 Oropharyngeal Dysphagia

Oropharyngeal dysphagia is related to difficulty or discomfort passing a bolus within the oral cavity or the pharynx. It may result from structural alterations that can impede bolus progression. These impediments include tumors and stenosis. [6]. Although structural defects can cause oropharyngeal dysphagia, it is more commonly caused by a functional disorder. Older individuals are more likely to experience oropharyngeal dysphagia. For a healthy subject, the duration of the pharyngeal swallow response is between 0.6 seconds and 1 second. The duration of the pharyngeal swallow response in older subjects is significantly longer than in healthy subjects due to delay in the early phase of oropharyngeal reconfiguration from a respiratory to a digestive pathway [6, 7, 8]. Patients with neurological diseases have an increased risk to develop oropharyngeal dysphagia. Other causes of oropharyngeal dysphagia include traumatic brain injuries, advanced Parkinson disease, multiple sclerosis, and individuals with head or neck injuries [1, 9].

1.1.2.1 Prevalence

Oropharyngeal dysphagia affects 30-40% of the population over 65 years old. In people over 65 years old, oropharyngeal dysphagia is present in 16 million Americans, 30 million Europeans, and 10 million Japanese individuals [1]. The prevalence of feeding difficulties, which can be an indicator of oropharyngeal dysphagia, is between 40% and 60% for institutionalized individuals, such as residents of assisted living facilities or nursing homes. The prevalence of oropharyngeal dysphagia in independently living individuals over 50 years old is estimated between 15% and 22%. Likewise, the estimated prevalence for independently living individuals between age 70 and 79 is estimated at 16.6%, while the estimated prevalence for individuals over age 80 is estimated at 33% [10, 11]. 64%-78% of stroke patients develop oropharyngeal dysphagia during the acute phase, and 40%-81% develop oropharyngeal dysphagia during the chronic phase. Up to 82% of patients with Parkinson's disease and up to 84% of patients with Alzheimer's disease experience oropharyngeal dysphagia [1, 6].

1.1.2.2 Symptoms

Individuals with oropharyngeal dysphagia often present overt symptoms. These symptoms include coughing or choking, difficulty swallowing, or pain associated with swallowing. Less obvious symptoms may also be present in a patient experiencing oropharyngeal dysphagia. These symptoms include delayed swallow initiation and excessive post-swallow residue which requires repeated swallows for pharyngeal clearance [12]. The symptoms present from oropharyngeal dysphagia occur within the oral and pharyngeal regions. Correct classification of dysphagia, whether esophageal or oropharyngeal, can be correctly distinguished 80 to 85% of the time with patient history and a physical examination [2, 13].

1.1.2.3 Complications

Oropharyngeal dysphagia can lead to a wide range of adverse outcomes, especially in elderly patients. Complications of untreated oropharyngeal dysphagia include weight loss, nutritional deficiency, and pneumonia. Patients with nutritional deficiency and dehydration are at a high risk of morbidity and mortality. Rehabilitative care and strict nutritional regiments are required for elderly and stroke patients. After a stroke, 45% to 68% of patients die within 6 months, largely due to nutritional and pulmonary complications resulting from oropharyngeal dysphagia [1, 12, 14].

1.1.2.4 Penetration Aspiration and Aspiration Pneumonia

Aspiration is one of the most common complications resulting from oropharyngeal dysphagia. Aspiration occurs when material is misdirected into the lower respiratory tract. When aspiration occurs, food or liquid passes beyond the true vocal folds and enters the trachea. The symptoms of aspiration are similar to the symptoms of oropharyngeal dysphagia, including coughing and choking. Symptoms of aspiration are not always overtly evident. Silent aspiration is defined when ingested material enters the respiratory system with no obvious indicators of aspiration. Silent aspiration is present in as much as 25% of acute stroke patients [15].

Aspiration pneumonia is not categorized as a distinct condition. Rather, aspiration pneumonia is grouped into the spectrum of pneumonia's, which are categorized by infection of the lungs. Symptoms of aspiration pneumonia are normally severe and develop within hours to days [16]. Aspiration pneumonia is associated with higher mortality rate compared with other forms of pneumonia. Results from a survey of over 1 million patients in more than 4200 hospitals concluded aspiration was present in 4% to 26% of pneumonia patients. The expected mortality rate from aspiration pneumonia is 29.4% versus 11.6% for other forms of pneumonia [16]. Aspiration pneumonia is the leading cause of death in patients with Parkinson disease, amyotrophic lateral sclerosis, and multiple types of dementia [1].

Penetration can be described as passage of food or liquid into the larynx that does not pass below the vocal folds. There exists a scale to describe penetration and aspiration in patients. This is an 8-point categorical scale known as the Penetration Aspiration Scale [17]. The Penetration Aspiration Scale rates penetration aspiration with an integer score from 1 to 8. A 1 on the scale demonstrates no observed penetration or aspiration, indicating a healthy swallow, while a score of 2-5 indicates penetration, and a score of 6-8 designates aspiration. The Penetration Aspiration Scale has been proven to reliably quantify select penetration and aspiration events observed during videofluoroscopic swallow evaluations [17].

1.1.3 Treatment of Dysphagia

1.1.3.1 Postural Strategies

Upright posture and symmetry are desirable during swallowing. Postural strategies are simple and effective, causing minimal fatigue. Anterior neck flexion, also known as the chin tuck maneuver, provides maximal airway protection when the head is flexed over the airway [6]. Figure 1 demonstrates the chin tuck maneuver. The chin tuck is utilized in patients when there is a delay in triggering the pharyngeal stage of swallowing or if there is reduced posterior movement of the tongue base [18]. It has proven effective in mild to moderate cases of dysphagia [19].

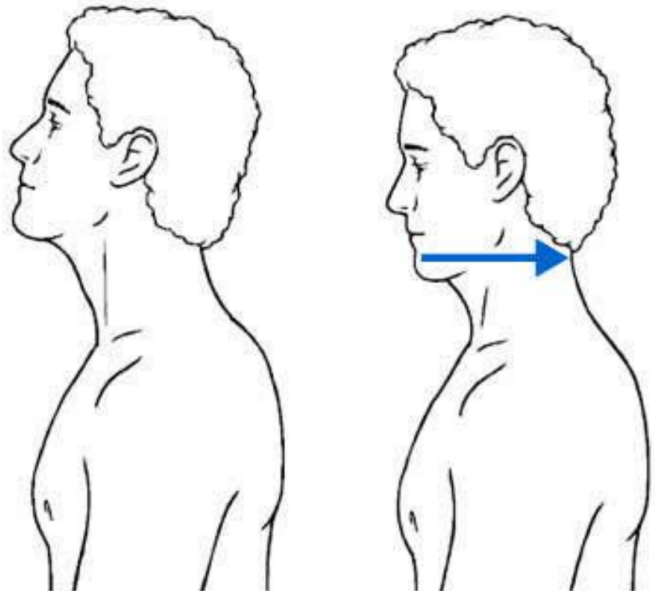

Figure 1: Chin Tuck Maneuver [18]

1.1.3.2 Specific Swallowing Maneuvers

Patients can learn and perform various maneuvers autonomously to compensate for biomechanical deficiencies. A supraglottic swallow aims to close the vocal folds before and during a swallow in order to protect against aspiration and cough immediately proceeding a swallow to clear residue. A forceful swallow aims to increase bolus propulsion. Double deglutition is useful in patients with post-swallow residue, as it can minimize residue before new inspiration [6].

1.1.3.3 Dietary Modifications

In neurological and older patients, reduction of bolus volume and improvement of bolus viscosity can significantly decrease penetration and aspiration [6]. Patients with decreased deglutition efficiency may require modification of liquid textures to maintain adequate hydration without penetration or aspiration. Using a thickening agent can prevent aspiration of thin liquid. [20].

1.2 Swallowing Physiology

Swallowing is a systematic, yet complex series of events in which food and liquid are transferred from the oral cavity to the stomach [21]. A swallow combines a variety of biomechanical processes. Swallowing requires precise mechanical and neurological coordination of over 30 muscles and nerves to guarantee a safe passage of materials through the upper aerodigestive tract [22]. Each swallow is divided into the oral preparatory phase, oral transport phase, pharyngeal phase, and esophageal phase. Precise coordination of kinematic events ensures the proper ingestion of a bolus and protection of the upper respiratory tract from unwanted particles [23].

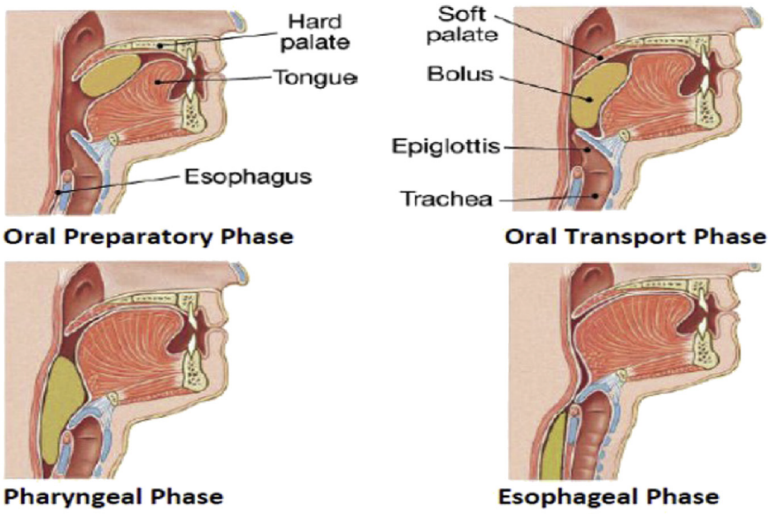

Figure 2: Anatomical Structures and Phases Involved in a Swallow [24]

1.2.1 Oral Preparatory Phase

The oral preparatory phase is identified by preparing a bolus. When solids are ingested, mastication mechanically breaks down solids and saliva assists in chemical break down of larger particles [24]. Initially, the bolus is held in the anterior portion of the oral cavity. During this process, the soft palate lifts to seal the nasopharynx as the tongue moves the bolus along the hard palate [25]. The duration of the oral preparatory phase is determined on bolus size and consistency.

1.2.2 Oral Transport Phase

The oral transport phase is identified as moving the bolus into the pharynx. The oral seal, nasopharyngeal seal, and the muscles of the tongue contract to move the bolus into the pharynx [24]. The posterior tongue depresses during this process to allow proper movement of the bolus. With ingestion of liquids, the pharyngeal phase begins during oral transport [22]. Thus, the oral transport phase is grouped into the oral preparatory phase when only liquid is present in the bolus.

1.2.3 Pharyngeal Phase

The pharyngeal phase is the most rapid phase of swallowing with complex, sequential operation required. In a healthy swallow, this phase should occur within one second. It performs two crucial operations: passage of the bolus and airway protection. The bolus is passed through the pharynx and upper esophageal sphincter to the esophagus, while the pharynx is separated from the larynx and trachea [22]. This phase begins with contraction of multiple muscles of the larynx, which closes the vocal cords and temporarily halting respiration [24]. This temporary halt of respiration prevents the bolus from entering the nasal cavity. The pharynx elevates and the tongue retracts, which moves the bolus towards the esophagus by use of peristaltic waves [26]. Meanwhile, the larynx and hyoid bone are raised. The epiglottis tilts backward to seal the larynx [22]. The seal of the larynx is crucial for airway protection. With the elevation of the pharynx and larynx, the upper esophageal

sphincter opens, and the bolus passes through. This designates the termination of the pharyngeal phase. Figure 3 displays the major features of the oral and pharyngeal phases of a healthy swallow.

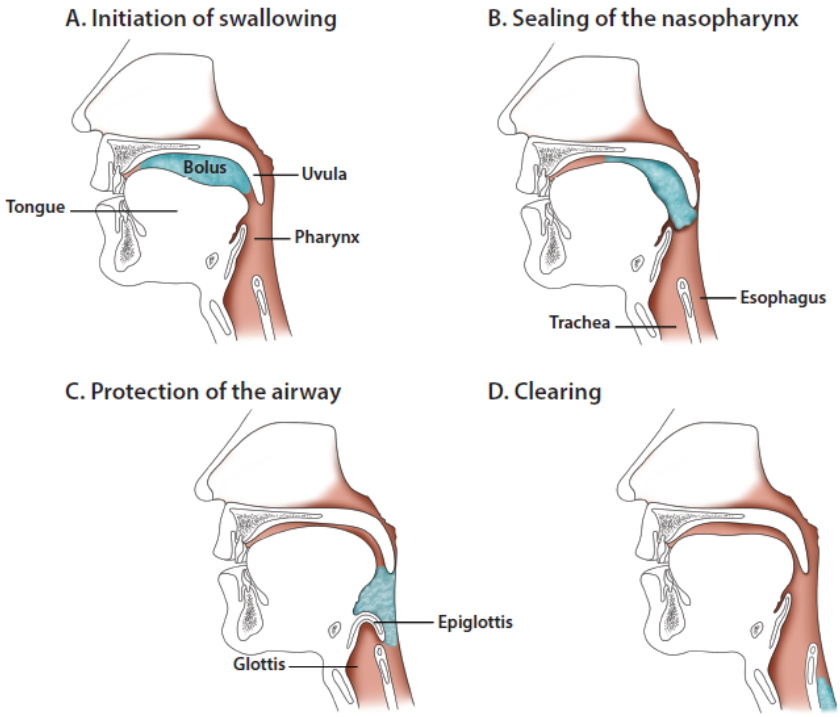

Figure 3: Major features of an Oropharyngeal Swallow [10]

1.2.4 Esophageal Phase

The esophageal phase consists of propulsion of the bolus through the esophagus to the stomach. In a healthy adult, the bolus should pass through the esophagus between 8 and 13 seconds [27]. The upper esophageal sphincter closes after passage of the bolus to prevent material from entering the larynx. A peristaltic wave propels the bolus through the lower esophageal sphincter to the stomach [22]. In an upright position, gravity assists in transport of the bolus through the esophagus to the stomach.

1.3 Swallowing Assessments for Dysphagia Diagnosis

Correct identification of dysphagia can be obtained with careful patient history and a physical examination [2, 13]. Although identification of dysphagia can be performed without more invasive methods, diagnosis cannot be made without a more comprehensive swallowing assessment. There are many diagnostic assessments available to diagnose esophageal dysphagia, and there are many diagnostic assessments and bedside screenings available to diagnose oropharyngeal dysphagia.

1.3.1 Upper Gastrointestinal Endoscopy

An upper gastrointestinal endoscopy is a procedure which utilizes a long, flexible tube known as an endoscope. Endoscopy is utilized in patients with dysphagia to determine etiology of the esophagus [28]. Often times, this examination is the first diagnostic used by many clinicians to diagnose esophageal dysphagia. An upper gastrointestinal endoscopy is almost always required in the evaluation of esophageal dysphagia [3].

1.3.2 High-Resolution Esophageal Manometry

High-resolution esophageal manometry assesses esophageal motility patterns by measuring the amplitude of contractile events in the esophagus and its sphincters in relation to time [29]. High-resolution esophageal manometry can be used to evaluate esophageal dysphagia. A thin, flexible catheter is inserted into a nostril, through the esophagus, and into the stomach. The catheter contains many solid-state sensors, equally spaced, to record esophageal contractions [30]. Patients may experience gagging and discomfort during the procedure, thus it is desirable for this examination to be as quick as possible.

1.3.3 Fiber-Optic Endoscopic Evaluation of Swallowing

Fiber-optic endoscopic evaluation of swallowing involves passing a fiber optic camera through the oropharynx to visualize the pharynx, larynx, and proximal trachea to diagnose

dysphagia. Fiber-optic endoscopic evaluation observes the patients anatomy and physiology in fine detail before and after the swallow to detect dysphagia [31]. The patient does not require any special substrates with fiber-optic endoscopic evaluation, rather, normal food can be used for a bolus. No x-ray imaging is required, meaning this examination can be performed bedside.

However, fiber-optic endoscopic evaluation is subject to multiple defects. The oropharyngeal anatomy is not fully visible to the clinician, resulting in a limited field of view. During the pharyngeal phase of swallowing, the pharynx collapses over the camera lens, meaning fiber-optic endoscopic evaluation cannot illustrate the actions of the pharynx and larynx during a swallow [31]. This evaluation is invasive; it normally requires topical anesthesia, which may drip into the oropharynx or larynx [32]. Insertion of a tube through the oropharynx can cause discomfort and gagging for the patient.

1.3.4 Videofluoroscopic Swallowing Study

A videofluoroscopic Swallowing Study (VFSS), also known as the modified barium swallow test, is considered the gold standard diagnostic tool to evaluate oropharyngeal dysphagia [33]. VFSS is a radiological diagnostic that provides a dynamic view of the oral cavity, pharynx, and upper esophagus during a swallow. The radiological images are obtained by administering barium-mixed boluses to the patients. The images can be taken from different views, such as lateral or anterior/posterior, to provide a complete summary of function. VFSS has been shown to accurately detect penetration and aspiration in a patient [34].

Similar to fiber-optic endoscopic evaluation, VFSS is subject to some defects to be categorized as a rapid, non-invasive diagnostic tool to diagnose oropharyngeal dysphagia. Availability of equipment and materials is critical to VFSS. This examination requires radiographical equipment, thus exposing a patient to x-ray radiation [34]. VFSS relies on barium swallows. Without barium-mixed substances, the bolus is radio-translucent, making kinematic analysis impossible.

VFSS cannot be performed bedside, making bedside screening unavailable and early detection less likely. VFSS uses the Penetration Aspiration Scale to rate swallows. Penetration

aspiration scores can be subjective from clinician to clinician. Traditional VFSS usually employs the judgment of at least two clinicians. Studies suggest that even in ideal conditions, well-trained blinded evaluators frequently report inconsistent and inaccurate subjective assessment of VFSS parameters [33]

1.3.5 High Resolution Cervical Auscultations

High resolution cervical auscultation (HRCA) is an emerging method that has been recently utilized as a less expensive and non-invasive swallowing assessment tool. HRCA involves the use of a 3-dimensional accelerometer to record vibrations and a contact microphone to record sound induced by the swallowing process.

Raw HRCA signals in real-time are not studied by clinicians due to inconsistency from movement, coughing, speaking, or external vibrations [35, 36]. Although real-time and manual interpretation of the un-processed HRCA data is unreliable, preceding studies utilizing advanced signal processing, and machine learning techniques have presented preliminary evidence of the precision of HRCA signals in the detection of swallowing kinematic events and penetration-aspiration [37, 38, 39, 40, 41, 42]. For instance, HRCA has been proven to accurately track the hyoid bone during swallowing without assistance or supervision from human experts [41], in addition to the detection of critical physiological events such as the upper esophageal sphincter opening and laryngeal vestibule closure [42, 43].

Despite of the success achieved by HRCA in swallowing assessment, it relies mainly on thin liquid barium swallows performed in conjunction with VFSS. This criteria subjects HRCA to similar issues arisen from VFSS, including availability of equipment and exposure to x-ray radiation. With reliance on VFSS to properly utilize HRCA, bedside screening is not possible.

1.3.6 The Toronto Bedside Swallowing Screening Test

The Toronto Bedside Swallowing Screening Test is a bedside swallowing screening first developed to identify patients at risk for dysphagia following a stroke. The Toronto Bedside Swallowing Screening Test is comprised of four tests, which include: Kidd water swallow

test (50mL water test), pharyngeal sensation, tongue movement, and general dysphonia [44]. General dysphonia is comprised of two items: patient voice before and patient voice after assessment. Along with the tests, there is a response grid completed by the nurse. The Toronto Bedside Swallowing Screening Test utilizes pass/fail scoring for each item, and administration continues only until the first failed item [44]. The assessment is completed in approximately 10 minutes, however, the assessment for a patient with severe dysphagia will likely result in a shorter assessment. Failure of the Toronto Bedside Swallowing Screening Test results in prompt referral to a speech language pathologist or a dysphagia expert.

In a clinical study, the Toronto Bedside Swallowing Screening Test achieved overall sensitivity of 91.3% across all settings and negative predictive values of 93.3% in acute patients and 89.5% in rehabilitation patients [44]. The ability of this examination to identify patients at risk for dysphagia is excellent, however, it is subject to three main issues. Patients should only perform the assessment who are alert, able to sit upright, and are able to follow simple instructions. Patients without full cognitive ability, such as recent stroke victims, should not immediately be screened using this examination. The Toronto Bedside Swallowing Screening Test is performed bedside by healthcare professionals, routinely nurses. Before a healthcare professional can administer the test, a 4 hour didactic session is required, in addition to interpretation of the Toronto Bedside Swallowing Screening Test using digitized real-life examples of 5 stroke patients [44]. Lastly, failure of the screening does not confirm a diagnosis for dysphagia, rather a failure directs the patient to more specialized care for proper diagnosis and treatment, if required. Therefore, the Toronto Bedside Swallowing Screening Test cannot be considered an all-encompassing bedside screening to diagnose dysphagia.

1.3.7 3-Ounce Water Swallow Test

The 3-ounce water swallow test is frequency used to determine patient risk of oropharyngeal dysphagia and aspiration. The test requires a patient to perform a swallow with 3 ounces of water without interruption. A failure of the test is indicated by any of the 3 following qualities: inability to complete the swallow, presence of coughing or choking, or a wet-hoarse vocal quality displayed during or within 1 minute of swallow completion [45].

An investigation of the clinical usefulness of the 3-ounce water swallow test determined the overall accuracy was only 59.7% with sensitivity of 96.5% and specificity of 48.7%. The false positive rate was 51.3%, while the false negative rate was 3.5% [45]. The high false negative rate/low specificity means more than half of all patients who fail the water swallow test will be unnecessarily referred to a speech language pathologist. As patients with silent aspiration do not exhibit explicit signs of dysphagia, the 3-ounce water swallow test can misdiagnose these patients. Like the Toronto Bedside Swallowing Screening Test, the 3-ounce water swallow test cannot confirm a diagnosis for aspiration or oropharyngeal dysphagia, rather, a more comprehensive diagnostic test must be performed when a patient fails the test. Given these issues, the 3-ounce water swallow test cannot be considered an accurate and definitive bedside evaluation to diagnose dysphagia.

1.3.8 Yale Swallow Protocol

The Yale Swallow Protocol is a bedside dysphagia screening to identify patients with swallowing problems and at risk for aspiration. A patient will be excluded from the Yale Swallow Protocol if the risk is too high. The screening consists of 3 phases. The first phase is a brief cognitive screening to ensure patient awareness. The second phase is an oral mechanical exam in which the administrator looks for overt signs of dysphagia, such as facial symmetry and tongue range of motion. The third phase consists of the 3-ounce water swallow test [46].

Studies show the Yale Swallow Protocol achieves 98% accuracy, 96.5% sensitivity, and 97.9% negative predictive value [46]. This means the screening can almost always assign a positive result to patients who aspirate and give a negative result to a patient that does not aspirate. However, this screening cannot confirm diagnosis of oropharyngeal dysphagia; it only warrants further examination from a speech language pathologist.

1.3.9 The Modified Mann Assessment of Swallowing Ability

The Mann Assessment of Swallowing Ability is a bedside dysphagia screening initially developed for first-time stroke patients. However, this examination is frequently utilized on

non-stroke patients to estimate the risk of aspiration and dysphagia severity [47]. The Mann Assessment of Swallowing Ability consists of 24 clinical items from 4 categories: general patient examination and the first 3 phases of swallowing (oral preparatory, oral transport, and pharyngeal phases). The maximum possible score is 200 points, with a score lower than 177 indicating dysphagia. A lower score indicates a higher risk of aspiration and higher severity of dysphagia [47].

The Modified Mann Assessment of Swallowing Ability includes 12 of the 24 items found in the Mann Assessment of Swallowing Ability. The maximum possible score on this examination is 100 points, with a lower score indicating a higher likelihood of aspiration [48]. A study confirmed the sensitivity, specificity, predictive values, and false-positive and false-negative rates are adequate for an initial evaluation for dysphagia. The discovered reliability across clinicians, namely neurologists, was high because the Modified Mann Assessment of Swallowing Ability incorporates general medical and neurological knowledge [48]. However, this examination is subject to multiple defects. Most of the tools proposed have been designed for use by speech language pathologist, meaning many items will require special expertise or training in protocol administration. The Modified Mann Assessment of Swallowing Ability only has the ability of to determine a if patient requires further diagnostic evaluation to confirm a diagnosis of dysphagia. Therefore, the Modified Mann Assessment of Swallowing Ability cannot be considered an accurate, definitive, or readily available diagnostic evaluation for bedside dysphagia diagnosis.

1.4 Thesis Scope

Despite the ability of many bedside dysphagia screenings to correctly identify the risk of dysphagia, these assessments necessitate additional diagnostic examinations to confirm a diagnosis. The Toronto Bedside Swallowing Screening Test and the Mann Assessment of Swallowing Ability require clinician training to properly administer [44, 48]. Fiber-optic endoscopic evaluation can be performed bedside, however, it is invasive, can cause discomfort for the patient, and does not provide a comprehensive field of view during deglutition

[32, 31]. VFSS has been proven to accurately detect dysphagia and aspiration, however, radiographical equipment and material to create contrast (such as thin liquid barium) is required analysis. Thus, VFSS cannot be performed bedside. In addition, scoring between raters has been shown to be inconsistent [33].

Despite of the success achieved by HRCA in swallowing assessment, it relies mainly on barium swallows performed in conjunction with VFSS. On the other hand, most bedside screening procedures are water-based tests, which do not involve the use of barium boluses. For HRCA to be proven effective for swallowing screening, it has to produce clinical insights for water swallows as accurately as it does for barium swallows. Using water swallows with VFSS is not of merit as water is radiolucent and the bolus path does not show up on VFSS, making the kinematic analysis infeasible. One way to achieve HRCA water-based bedside screening is to train the machine learning algorithms using HRCA signals from the well rated barium-based swallows and use the algorithms on HRCA signals from water-based swallows directly. However, this can be valid if and only if HRCA signals don't present significant differences between water-based and barium-based swallows.

This study investigates the patterns emerging from HRCA signals when using thin liquid barium swallows in comparison with water swallows. It is hypothesized that HRCA signals will present no strong variations between water and thin liquid barium swallows given the close values of the consistency of both materials. To verify this hypothesis, water and thin liquid barium swallows were collected from healthy participants and statistical significance tests were performed to determine the significantly different HRCA signal features between the two types of swallows. Further, classification models were trained to differentiate between the two types of swallows based on HRCA signal features which, if successful, points out that there exist dissimilarities between the two types of swallows

1.5 Thesis Contributions

An HRCA bedside evaluation performed with water possesses numerous advantages to all other diagnostic and investigatory examinations. It can be performed by any trained medical professional, is non-invasive and inexpensive, does not require any training, can be promptly conducted, and does not require an immediate follow up test to confirm dysphagia. This study is a preliminary investigation into the validity of using water as the swallowing material for an HRCA bedside evaluation. If the hypothesis that no strong variations present between water and thin liquid barium swallows is confirmed, this study will be verified with a larger patient population.

1.6 Thesis Structure

Chapter 2 describes the mathematical background of statistical significance testing and machine learning algorithms: linear mixed models, linear support vector machines (SVM), Naïve Bayes classification, K-means clustering, and dimensionality reduction with principal component analysis (PCA). Chapter 3 presents the methodology used in this study, including signal pre-processing and mathematical background of the extracted features. Chapter 4 discusses the results of the statistical models and machine learning classifiers. Chapters 5 and 6 include a discussion of the results, conclusions drawn from analysis, and future experimentation into this subject.

2.0 Background

2.1 Statistical Significance Testing

Statistical significance testing was performed in this study using linear mixed models. A linear mixed model helps to determine the association between two variables with the assumption that all observations are independent and identically distributed. Linear mixed models can be represented with the following equation:

$$y = x\beta + Zu + \epsilon \tag{1}$$

where y is the predicted output, x is the input, β represents the fixed-effect regression coefficients, Z and u represent random effects, and ϵ represents information not explained in the model [49].

A linear mixed model can include a t-test, which is used to determine if there is a significant difference between the mean of two variables. The test will assume Gaussian distributions, simplifying the calculation of the p-value, which is the probability under the null hypothesis that an observation is as or more extreme than the observed value. The threshold for significance α is normally set at 0.05. If the p-value is less than α, the null hypothesis is rejected, and the variables are determined to have correlation.

2.2 Machine Learning Classifiers

Machine learning algorithms use statistics to find patterns in data. In its simplest form, a machine learning algorithm uses data (often referred to as training data) to train an algorithm. This trained algorithm is used to predict the class label for a separate data set, known as testing data.

This study aimed to distinguish between the HRCA signals emanating from a barium swallow and HRCA signals emanating from a water swallow. To make this distinction, binary

machine learning classifiers were utilized. In a binary machine learning classifier, the dataset contains two distinct classes. In this study, one class represented a barium swallow and the other class represented a water swallow. This study analyzes swallowing data with three distinct binary classifiers, including a support vector machine, Naïve Bayes classification, and K-means clustering.

Dimensionality reduction transforms high dimensional data onto a lower dimensional space while retaining as much information about the original data as possible. It is important to utilize dimensionality reduction for two reasons. First, ultra high dimensional data sets or data sets with many observations can be computationally expensive. Dimensionality reduction techniques can decrease computation time. Next, some features within a data set may not provide useful information to correctly classify data. Although dimensionality reduction speeds classification, it can contribute to loss of information. This study utilizes principal component analysis for dimensionality reduction. In the case of this research, PCA cannot determine which HRCA features provide important information on swallowing kinematics. Thus, the machine learning classifiers must be analyzed with and without principal component analysis to determine if dimensionality reduction alters the information content of the collected signals.

2.2.1 Support Vector Machines

The support vector machine (SVM) is a supervised learning algorithm, meaning the labels of training (or input) data must be known to predict the labels of the testing data. It is a linear, binary maximum margin classifier [50]. A maximum margin classifier aims to maximize the distance between the decision boundary and any of the training data points. A support vector machine can be characterized generally by the following equation:

$$y(x) = w^T \phi(x) + b \tag{2}$$

where w is a vector of weights, $\phi(x)$ is a fixed feature-space transformation, and b is a constant bias term. The training data consists of N distinct vectors $(x_1, x_2, ..., x_n)$ with corresponding labels of $(y_1, y_2, ..., y_n)$ where $y_n \epsilon \{-1, 1\}$.

The distance of a data point, x_n, to the decision plane is:

$$\frac{y_n(w^T\phi(x_n)+b)}{||w||} \tag{3}$$

The margin is defined as the perpendicular distance between the decision plane and the closest data point. The location of the decision plane is determined by support vectors, which are a subset of data points closest to the decision plane. A simple representation of a support vector machine, margin, and support vectors are depicted in figure 4, with circles indicating support vectors.

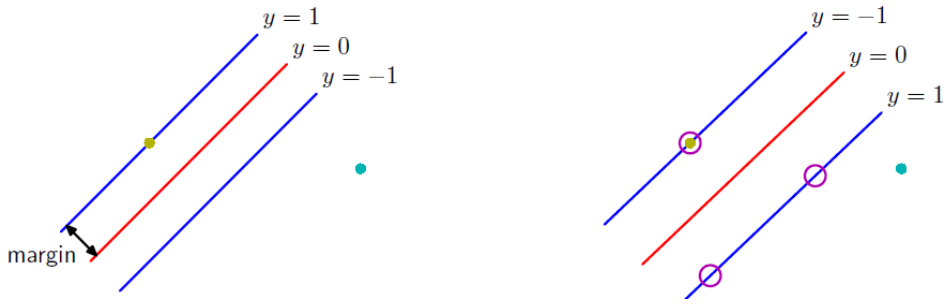

Figure 4: Depiction of A Two Dimensional Support Vector Machine [50]

The objective with support vector machines is to maximize the margin in equation 3, which corresponds to optimization of the parameters w and b, while satisfying the constraint: $y_n(w^T\phi(x_n)+b) \geq 1$ [50], which leads to the following constrained optimization problem:

$$\begin{aligned} &\textit{maximize} && \tfrac{1}{2}||w||^2 \\ &\textit{subject to} && 1 - y_i(w^T\phi(x_i)+b) \leq 0 \end{aligned} \tag{4}$$

Using Lagrange multipliers (with the Lagrange multipliers designated by α_i) yields the following dual equation:

$$\begin{aligned} &\textit{maximize} && \textstyle\sum_{i=1}^n \alpha_i - \frac{1}{2}\sum_{i,j=1}^n \alpha_i\alpha_j y_i y_j \phi(x_i^T)\phi(x_j) \\ &\textit{subject to} && \textstyle\sum_{i=1}^n \alpha_i y_i = 0 \\ & && \alpha_i \geq 0 \end{aligned} \tag{5}$$

After solving for all Lagrange multipliers, the weight vector and bias term, w and b, are determined with the following equations:

$$w = \sum_{i=1}^{n} \alpha_i y_i x_i \tag{6}$$

$$b = \frac{1}{N} \sum_{i=1}^{n} \Big(y_i - \sum_{j=1}^{n} \alpha_j y_j \phi(x_i^T) \phi(x_j) \Big) \tag{7}$$

Finally, each test data point, designated by x, is classified utilizing every training data point, designated by x_i, using the following equation:

$$y(x) = sgn\Big(\sum_{i=1}^{n} a_i y_i \phi(x) \phi(x_i) \Big) \tag{8}$$

where data points are classified according to the position in relation to the decision boundary. If a test data point is "above" the boundary, it is assigned to the positive class, whereas a point "below" the boundary is assigned to the negative class.

A linear support vector machine performs well with data that is linearly separable. The decision boundary of N dimensional data is an N-1 dimensional hyperplane. Utilizing the equations to calculate the ideal hyperplane for the decision boundary, new data to be tested by the support vector machine should be correctly classified.

2.2.2 Naïve Bayes Classification

Naïve Bayes classification is a probabilistic classifier based on Bayes theorem, which assumes all features are independent given its class [50]. Naïve Bayes classifiers can be used for multi-class problems, however, this application only requires binary class labels. Like a SVM, Naïve Bayes classification requires labeled data. Given input, x, and the corresponding label, C_k, Bayes theorem states [51]:

$$p(C_k|x) = \frac{p(C_k)p(x|C_k)}{p(x)} \tag{9}$$

where $p(x)$ can be treated as a constant. The numerator, $p(C_k)p(x|C_k)$, is equivalent to $p(C_k \cap x)$ by the definition of conditional probability [51], which can then be re-written as: $p(x_1 \cap x_2 ... \cap x_n \cap C_k)$. Using the chain rule applied with conditional probability

theory along with the assumption of conditional independence, this term simplifies to: $p(C_k)p(x_1|C_k)p(x_2|C_k)...P(x_n|C_k) = p(C_k)\prod_{i=1}^{n} p(x_i|C_k)$. This leads to the following decision rule utilized by a Naïve Bayes classifier:

$$\hat{y} = \underset{C_k}{\operatorname{argmax}}\, p(C_k) \prod_{i=1}^{n} p(x_i|C_k) \tag{10}$$

where $\hat{y}$ is the assigned class label with $C_k \epsilon \{1, 2\}$ for a binary classifier.

Naïve Bayes classification operates given the principle that all features are independent. However, this study utilizes features that are likely dependent. For example, the time domain features in the anterior-posterior direction for a swallow completed with barium can likely exhibit dependence. For this reason, this classifier may not be ideal for this application. However, Naïve Bayes classification is easy to implement with minimal training data, thus it is utilized in this study.

2.2.3 K-Means Clustering

K-means clustering is a machine learning classification technique to identify clusters of data points in multi-dimensional space. The objective is to separate the data set into K clusters [50]. A cluster can be described as a group of data points in which the distance between points within a cluster is significantly less than the distance from a point to outside the cluster. K-means is traditionally used as an unsupervised learning algorithm, meaning class labels are not required for training data. However, it can be utilized as a supervised algorithm to verify a hypothesis on data in question.

For each data point x_n, binary indicators, $r_{nk} \epsilon \{0, 1\}$, are introduced with $k = 1, ..., K$ where k is the number of clusters. If a data point belongs to cluster k, then $r_{nk} = 1$ and $r_{nj} = 0$ for $i \neq j$. An objective function, which represents the sum of squares of the distance of each data point to the center of the cluster, is defined as:

$$J = \sum_{n=1}^{N} \sum_{k=1}^{K} r_{nk} ||x_n - \mu_k||^2 \tag{11}$$

where μ_k is the center of each cluster. This process becomes an optimization problem in which the aim is to find values for r_{nk} and μ_k that minimize the objective function, J [50].

First, each data point must be assigned to a cluster. This is achieved with optimization of the objective function in regards to r_{nk}. Assuming observations are independent, data points are assigned to the closer cluster center using the following equation:

$$r_{nk} = \begin{cases} 1 & if k = arg\ min_j ||x_n - \mu_j||^2 \\ o & otherwise \end{cases} \tag{12}$$

The derivative of the objective function is then taken with respect to μ_k and set to zero while holding r_{nk} fixed, yielding the following equation:

$$2\sum_{n=1}^{N} r_{nk}(x_n - \mu_k) = 0 \tag{13}$$

which simplifies to:

$$\mu_k = \frac{\sum_{n=1}^{N} r_{nk} x_n}{\sum_{n=1}^{N} r_{nk}} \tag{14}$$

After solving for the center of each cluster μ_k, all data points are re-assigned to the closest cluster. The process is repeated until there is no change in the cluster assignments for any training data points.

Once optimal values for μ_k are determined, the testing data can be assigned to clusters. Each test data point is assigned to a cluster using the following equation, which utilizes Euclidean distance as the performance metric:

$$\hat{y} = \underset{k}{\text{argmax}}\ \sqrt{(x - \mu_k)^2} \tag{15}$$

K-means clustering performs well with data that is distinctly separable in at least 1 dimension. In addition, data that is separable in multiple dimensions is likely to perform well with clustering techniques. As K-means clustering assigns data to K distinct clusters, K-means clustering algorithms will perform with high accuracy if the training data set is easily separable. This assertion is demonstrated in figure 5, which illustrates the iterative process of determining cluster centers for two dimensional data with $K = 2$.

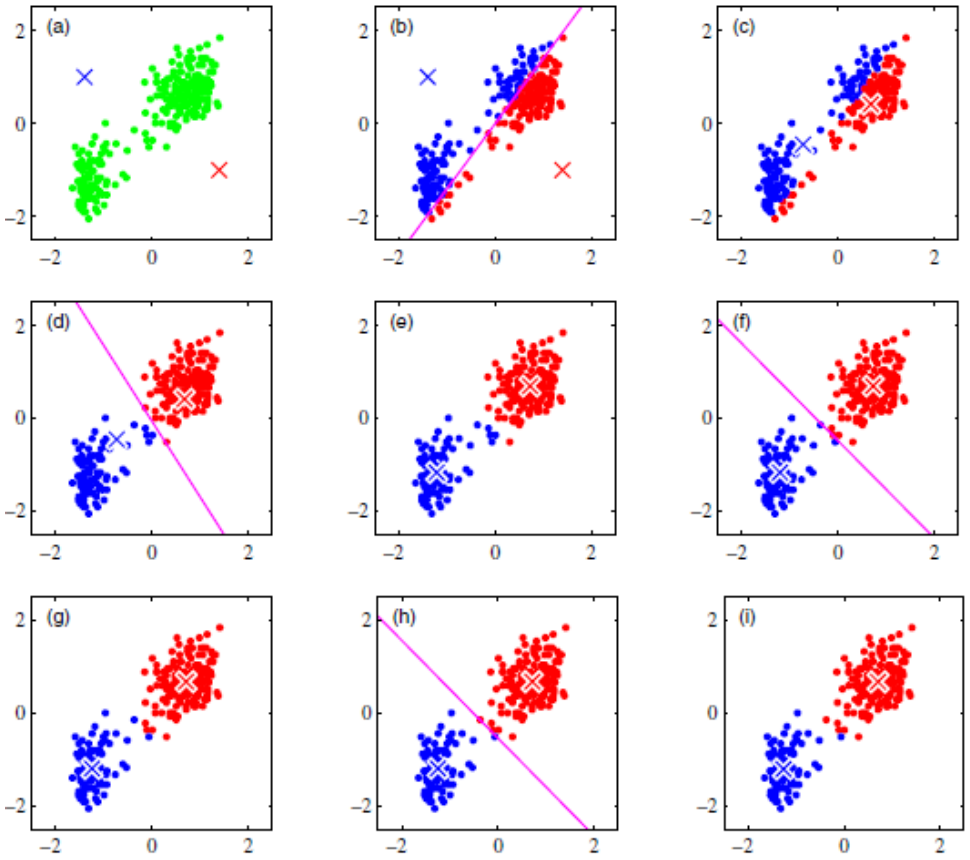

Figure 5: Iterative Process of K-means Algorithm with $K = 2$ [50]

2.2.4 Principal Component Analysis

Principal component analysis (PCA) is a technique for dimensionality reduction. PCA is used with machine learning classifiers to create lower dimensional data while preserving as much variability as possible from the original data set. It is the orthogonal projection of data onto a lower dimensional linear space such that the variance of the projected data is maximized [50]. An example of principal component analysis is illustrated in figure 6, where the original data set is 2-dimensional, which is represented by red dots, and the transformed data is projected onto a 1-dimensional space, which is represented as green dots.

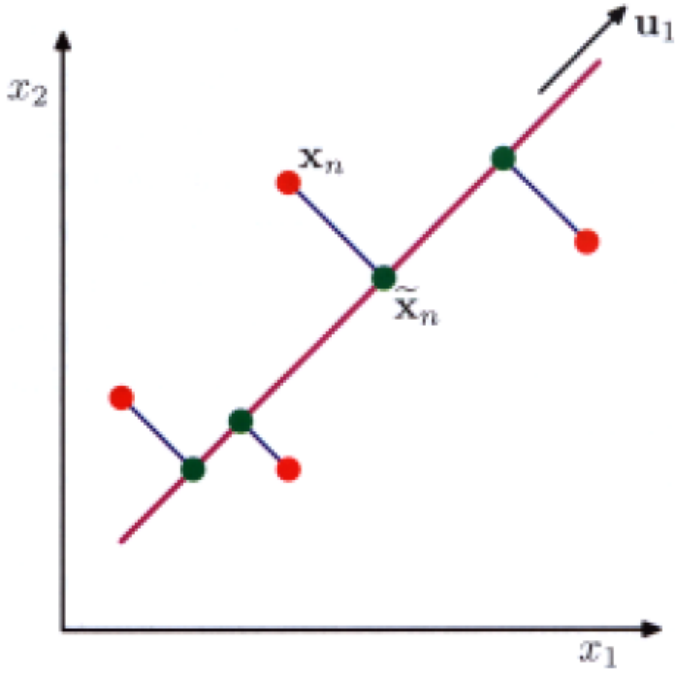

Figure 6: Visual Representation of Principal Component Analysis

Given N data points and each data point x_n with dimensionality d, the data is centered (or normalized) using the following equation:

$$A = x - \frac{1}{N}\sum_{n=1}^{N} x_n \tag{16}$$

The covariance matrix of the input data is formed using: $\Sigma = AA^T$. To solve for the eigenvalues λ_i of Σ, the following equation is used: $det(\Sigma - \lambda I = 0)$. Using the fundamental property of eigenvectors: $\Sigma U = \Lambda U$, where U is an $n \times n$ matrix with its i^{th} column corresponding to eigenvector q_i, and Λ is a diagonal matrix whose elements correspond to eigenvalues λ_i, the corresponding eigenvectors u_i are determined. The eigenvalues and corresponding eigenvectors for $\Sigma : \{\lambda_i, u_i\}$ $with$ $i = 1, 2, ..., d$ are determined and sorted from largest to smallest.

To determine the number of principal components, there are two common options. A scree plot displays the eigenvalues from largest to smallest. The number of principal components is chosen near the 'knee' of the curve or when the rate of decrease in eigenvalues falls below a given threshold. An example scree plot is illustrated in figure 7.

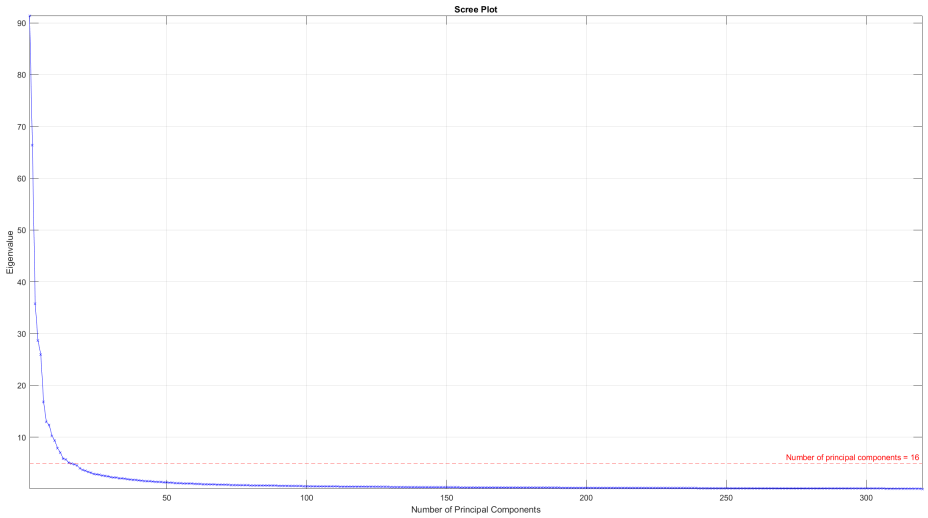

Figure 7: Example Scree Plot

In this study, the method to determine the number of principal components utilizes the percentage of total variance explained. The objective of this method is to explain as much variance in the training data while minimizing dimensionality. Traditionally, 95% is the minimum threshold for this method. The eigenvalues illustrate how much variance can be explained by its associated eigenvector. Therefore, the following equation is used to determine the variability explained by each principle component:

$$VarExplained_k = \frac{\lambda_k}{\sum_{i=1}^{d} \lambda_i} \times 100\% \tag{17}$$

The k largest eigenvalues are chosen such that $VarExplained \geq 95\%$. The corresponding eigenvectors create a basis for the projection of the data onto a lower dimensional space with matrix T [50]. The final transformation is computed using the following equation:

$$x_{new} = AT \tag{18}$$

where x_{new} is the input data transformed to a lower dimension, A is the centered training data, and T is the matrix of eigenvectors of the covariance matrix Σ. It is important to note that the same transformation T must be applied to the centered testing data.

Principal component analysis is not a standalone classification technique. However, PCA is useful to reduce the complexity of high dimensional data before use in a machine learning classifier, such as the three described in previous sections. With dimensionality reduction using principal component analysis, classification will require less computational power and can be less visually complex. Although useful for faster and more efficient computations, principal component analysis will remove information contained in the original data set, so results obtained from classifiers must be carefully examined before making assessments.

3.0 Methodology

3.1 Participants and Study Protocol

This study was approved by the institutional review board of the University of Pittsburgh. All participants provided written informed consent prior to enrollment. Water and barium swallows were collected from 36 community dwelling healthy adults (19 males, 17 females, age 66 $\pm$ 8). Participants reported no history of swallowing-related disorders. Each participant performed 5 VFSS free water swallows and 5 thin liquid barium swallows. 5 thin liquid barium swallows were discarded either due to poor HRCA signal quality or adverse swallowing conditions, such as existing residue before swallow. Each barium swallow involved ingestion of 3 mL of Varibar thin by spoon. The target viscosity of Varibar thin will not exceed 15 centipoise, which was determined as a part of a larger experiment [52]. Each water swallow involved ingestion of 3 mL by spoon. The researcher administered the bolus for each swallow, and the participants were instructed to, "Hold the liquid in your mouth and wait until I tell you to swallow it" and to perform all the swallows in neutral head position.

In total, 269 swallows were collected for this study (114 barium and 155 water). Participant data and total swallow statistics are illustrated in table 1 Analyzed data was only included from participants with multiple swallows from both barium and water. 5 additional barium swallows were excluded from analysis due to corrupted or unclear VFSS. This resulted in 185 swallows included in analysis for this study (90 barium and 95 water). This data is illustrated in Table 2.

3.2 Data Acquisition

In this study, we considered swallows with two different types of materials: water and thin liquid barium. For water swallows, only HRCA signals were collected. For thin liquid

Table 1: Participant Data and Total Swallows

Study Characteristics	
Total Participants	36
Male	19
Female	17
Age Range	50 to 87
Total Swallows	269
Barium	114
Water	155

Table 2: Analyzed Swallow Data

Swallow Data	
Number of Participants	19
Number of Swallows	185
Barium	90
Water	95

barium swallows, HRCA signals were collected simultaneously with VFSS. A standard fluoroscopy machine (Precision 500D, GE Healthcare, LLC, Waukesha, WI) was used for the barium thin swallows with a pulse rate of 30 PPS. A frame grabber card (AccuStream Express HD, Foresight Imaging, Chelmsford, MA) was used to capture and digitize the video output of the fluoroscopy machine at a rate of 73 frames per second. The same HRCA collection equipment was utilized for both types of swallows and used the same hardware setup in prior studies [42, 53]. A contact microphone (model C411L, AKG, Vienna, Austria) and a tri-axial accelerometer (ADXL 327, Analog Devices, Norwood, Massachusetts) were attached to the subjects' anterior neck. The accelerometer was placed over the cricoid cartilage where it was proven to produce the best signal quality [54]. The main accelerometer axes were perpendicular to the coronal plane (anterior-posterior), parallel to the cervical spine (superior-inferior), and parallel to the axial-transverse plane (medial-lateral). The microphone was placed slightly over the suprasternal notch towards the right lateral side of the larynx. Resultant signals were hardware bandpass filtered from 0.1 to 3000 Hz [55]. The signals were then digitized at 20kHz utilizing a National Instruments 6210 DAQ.

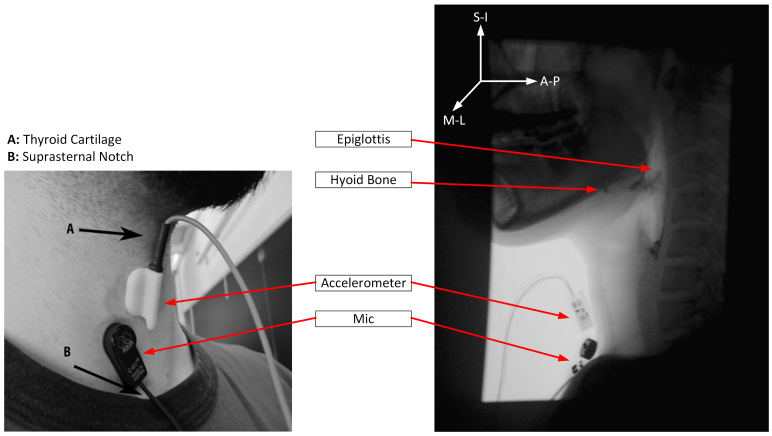

Figure 8: Placement of the tri-axial accelerometer and contact microphone

National Instruments' LabView was used to synchronize the streaming from all sensors and fluoroscopy machine and save the streams into the hard drive. Two separate programs were implemented in LabView to perform both thin liquid barium swallows with VFSS and VFSS free water swallows. The first program recorded continuously from the HRCA

sensors and the fluoroscopy machine with complete end-to-end synchronization to guarantee alignment of swallowing segments in both VFSS videos and HRCA signal records in barium thin swallows. The second program recorded only from the HRCA sensors for water swallows with an extra functionality that was used to roughly capture the onset and offset of the swallows. A push button was programmed to capture the time when pressed, was used by an observer who pressed it when the researcher gave the "swallow it" verbal command marking the onset of the swallow and released it when the participant completed the swallow marking the offset of the swallow.

3.3 Videofluoroscopic Swallow Study Image Analysis

The onset and offset of barium thin swallows were extracted through the inspection of the VFSS frames. The onset was defined as the frame in which the bolus head passes the shadow of the posterior ramus of the mandible and the offset as the frame in which the hyoid bone completes motion associated with pharyngeal swallowing activity and the bolus is cleared from the video frame [42]. Three expert raters identified the onset and offset of the barium thin swallows in VFSS videos. All raters established a priori intra- and inter-rater reliability with intra-class correlation coefficients over 0.99 using videos that were not included in the dataset under investigation, in addition to being blinded to participant demographics, bolus conditions, and each other's ratings to avoid any bias.

3.4 Signal Preprocessing

All collected signals were downsampled to 4 kHz, which retains signal quality while smoothing out any unwanted movement or physiological events that occur during swallowing [55, 56, 57]. The onset and offset of barium swallows in HRCA signals were calculated based on the onset and offset frames annotated in VFSS videos through using the proper sampling conversion. The onset and offset of water swallows in HRCA signals were calculated based

on the start time and end time determined by the push button through using the proper sampling conversion. These equations are described in the proceeding sections.

The baseline noise of each sensor, also known as zero-input response of the sensor, was modeled using an auto-regressive model which was then used to generate finite impulse response (FIR) filters to remove the noise form each part of the HRCA signals (3 axes of acceleration and the sound signal from the mic) [57]. All three acceleration signals were individually processed using a 4th order least-squares splines algorithm to reduce low-frequency components produced by participant head movement [58, 59]. Lastly, all signals were denoised using a 10th order Meyer wavelet to reduce any remaining noise [60].

3.5 Segmentation of Barium Swallows

The start sample and end sample for each barium swallow was determined using the following equations:

$$Start\ Sample = \left\lfloor \frac{(frame_{onset} - 1) \times f_s}{f_{VFSS}} \right\rfloor + 1 \tag{19}$$

$$End\ Sample = \left\lfloor \frac{frame_{offset} \times f_s}{f_{VFSS}} \right\rfloor \tag{20}$$

where $frame_{onset}$ and $frame_{offset}$ correspond to the onset frame and offset frame identified in the VFSS video, $f_s = 4000\ Hz$ is the sampling frequency, and $f_{VFSS} = 73\ Hz$ is the frame rate of the VFSS video.

3.6 Segmentation of Water Swallows

The start sample and end sample for each water swallow was determined using the following equations:

$$Start\ Sample = \left\lfloor \frac{time_{start} \times f_s}{1000} \right\rfloor + 1 \tag{21}$$

$$End\ Sample = \left\lfloor \frac{time_{end} \times f_s}{1000} \right\rfloor \tag{22}$$

where $time_{start}$ and $time_{end}$ correspond to the start time and end time in milliseconds determined from the push button during data acquisition and $f_s = 4000\ Hz$ is the sampling frequency.

3.7 Feature Extraction

For a better representation of the HRCA signals, 9 features were extracted in 4 domains: time, information-theoretic, frequency, and time-frequency. Time domain features include: standard deviation, skewness, and kurtosis; information theoretic domain features include: Lempel-Ziv complexity and entropy rate; frequency domain features include peak frequency, spectral centroid, and bandwidth; and the time-frequency domain feature is wavelet entropy. All 9 features were extracted from each of the 4 recorded signals: swallowing sounds from the microphone (MIC), anterior-posterior acceleration (AP), superior-inferior acceleration (SI), and medial-lateral acceleration (ML) to investigate the similarities and differences between the HRCA signals of water and barium thin swallows. These 9 features have been utilized in preceding studies and are proven useful in analysis of swallowing [53, 61, 62, 63, 64]. Each of the 9 features was calculated independently in all 4 domains. All features are listed with a brief description in table 3.

3.7.1 Time Domain Features

The time domain gives insight into the behavior of a discrete time signal with n samples, $X = \{x_1, x_2, ..., x_n\}$. The three time domain features are as follows:

- **Standard deviation**

  Variance of a signal is defined as the average of the squared differences from the mean of a signal. The standard deviation of a signal is defined as the square root of its variance.

It can be calculated using the following equation:

$$\sigma = \sqrt{\frac{\sum_{i=1}^{n}(x_i - \bar{x})^2}{n-1}} \tag{23}$$

where $\bar{x}$ is the sample mean of the discrete time signal.

- **Skewness**

  Skewness is a measure of the asymmetry of a signal about its mean. It can be calculated using the following equation:

$$\gamma_1 = \frac{\frac{1}{n}\sum_{i=1}^{n}(x_i - \bar{x})^3}{\left[\frac{1}{n}\sum_{i=1}^{n}(x_i - \bar{x})^2\right]^{3/2}} \tag{24}$$

- **Kurtosis**

  Kurtosis describes the tailedness and peakness of a distribution relative to normal distribution. It can be calculated using the following equation:

$$\gamma_2 = \frac{\frac{1}{n}\sum_{i=1}^{n}(x_i - \bar{x})^4}{\left[\frac{1}{n}\sum_{i=1}^{n}(x_i - \bar{x})^2\right]^{2}} \tag{25}$$

3.7.2 Information-Theoretic Domain Features

The information-theoretic domain gives insight into the patterns exhibited by a discrete signal. Both features are as follows:

- **Lempel-Ziv complexity**

  The Lempel-Ziv complexity is a measure of the predictability of a signal. Before analysis, the signal should be transformed into a finite symbol sequence. Binary signals are traditionally employed for biomedical signals [65], however, this study uses 100 equally spaced quantization levels ranging from the minimum value to maximum value of the signal.

  Lempel-Ziv complexity counts the number of unique subsequences in the quantized symbol sequence. If a subsequence belongs to an already discovered sequence, it is not considered unique. The number of unique subsequences k is a measure of complexity of the signal [65]. A higher value of k designates a more complex signal. To obtain a

measure of complexity that does not depend signal duration (with n samples), the final expression for Lempel-Ziv complexity is as follows:

$$C = \frac{k \log_{100} n}{n} \tag{26}$$

- **Normalized Entropy rate**

  Entropy rate is a measure of the degree of regularity of a signal distribution. Initially, the signal is normalized to zero mean and unit variance using the mean and standard deviation, $\bar{x}$ and σ. The normalized signal is transformed using 10 equally spaced quantization levels represented by integers 0 through 9. Sequences in the quantized signal $\hat{X}$ of length L, $10 \leq L \leq 30$ are coded as a series of integers $\gamma_L = \{u_1, u_2, ..., u_{n-H+1}\}$ using the following equation:

$$u_i = \hat{x}_{i+L-1} 10^{L-1} + \hat{x}_{i+L-2} 10^{L-2} + ... + \hat{x}_i 10^0 \tag{27}$$

  The normalized entropy rate is computed using the following equation:

$$NER(L) = \frac{SE(L) - SE(L-1) + SE(1) perc(L)}{SE(1)} \tag{28}$$

  where $perc(L)$ is the percentage of elements in the sequence γ_L that are unique and SE is the Shannon entropy which is represented by the following equation:

$$SE(L) = \sum_{i=0}^{10^L - 1} p_{\gamma_L}(i) \ln p_{\gamma_L}(i) \tag{29}$$

  To give a measure for entropy rate between 0 and 1, $NER(L)$ was transformed into a measurement of regularity ρ [62]:

$$\rho = 1 - min(NER(L)) \tag{30}$$

  where $\rho = 0$ indicates a totally random signal, while $\rho = 1$ indicates a signal with maximum regularity.

3.7.3 Frequency Domain Features

The frequency domain gives insight into the behavior of signals by exploring the frequency spectrum of a discrete signal. The frequency spectrum of a signal is obtained from the Discrete Fourier Transform, designated as $F_X(f)$. The three frequency domain features are as follows:

- **Peak Frequency**

  The peak frequency of a signal corresponds to the frequency of maximum power. It is calculated using the following equation:

$$f_{peak} = \underset{f\epsilon(0,f_{max})}{\text{argmax}} \ \max |F_X(f)|^2 \tag{31}$$

  where $f_{max} = 2000\ Hz$ is limited by $\frac{1}{2}$ the sampling frequency $f_s = 4000\ Hz$ applied to the signal during data acquisition.

- **Spectral Centroid**

  The spectral centroid of a signal is defined as the center of mass of the frequency spectrum of the signal. It is calculated using the following equation:

$$\hat{f} = \frac{\int_0^{f_{max}} f|F_X(f)|^2 df}{\int_0^{f_{max}} |F_X(f)|^2 df} \tag{32}$$

- **Bandwidth**

  The bandwidth of a signal describes the range of frequencies over which the power density spectrum is concentrated. It is calculated using the following equation, which utilizes the spectral centroid:

$$B = \sqrt{\frac{\int_0^{f_{max}} (f-\hat{f})^2 |F_X(f)|^2 df}{\int_0^{f_{max}} |F_X(f)|^2 df}} \tag{33}$$

3.7.4 Time-Frequency Domain Features

The time-frequency domain simultaneously gives insight into the time and frequency domains of a discrete signal. The time-frequency feature analyzed in this study is as follows:

- **Wavelet entropy**

  Wavelet entropy is a measure of the disorderly behavior for non-stationary signal [66]. The relative energy in each wavelet decomposition level was extracted from a 10-level discrete wavelet decomposition of the signal using the discrete Meyer wavelet [60]. The decomposition can be designated as $W_x = [a_{10}, d_{10}, d_9, ..., d_1]$ with a_{10} representing the approximation signal and d_k representing the k^{th}-level detail signal. Signal energy can be approximated as:

$$E_{a_{10}} = ||a_{10}||^2 \tag{34}$$

$$E_{d_k} = ||d_k||^2 \tag{35}$$

  where $|| * ||$ is the Euclidian norm and $k = 1, 2, ..., 10$. The relative energy contribution from each decomposition level is:

$$Er_{a_{10}} = \frac{E_{a_{10}}}{E_T} \times 100 \tag{36}$$

$$Er_{d_k} = \frac{E_{d_k}}{E_T} \times 100 \tag{37}$$

  where E_T is the total energy of the signal:

$$E_T = E_{a_{10}} + \sum_{k=1}^{10} E_{d_k} \tag{38}$$

  Finally, the wavelet entropy is computed using the following [62] :

$$WE = -\frac{Er_{a_{10}}}{100} \log_2 \frac{Er_{a_{10}}}{100} - \sum_{k=1}^{10} \frac{Er_{d_k}}{100} \log_2 \frac{Er_{d_k}}{100} \tag{39}$$

Table 3: Summary of Features

Time Domain Features	
Standard deviation	Measure of a signal variance around its mean
Skewness	Measure of the asymmetry of a signal about its mean
Kurtosis	Describes the tailedness/peakness of a signal relative to normal distribution
Information-Theoretic Domain Features	
Lempel-Ziv Complexity	Measure of the randomness of a signal
Normalized Entropy rate	Measure of the degree of regularity of a signal distribution
Frequency Domain Features	
Peak frequency (Hz)	The frequency of maximum power
Spectral centroid (Hz)	The center of mass of the frequency spectrum of a signal
Bandwidth (Hz)	The frequency range of a signal
Time-Frequency Domain Features	
Wavelet entropy	Measure of the disorderly behavior for non-stationary signal

3.8 Data Analysis

In order to determine whether HRCA signals are different between water and thin liquid barium swallows, linear mixed models were created for each HRCA signal feature across all 4 signal axes. The linear mixed models show the statistical significance of each feature on differentiating between water and thin liquid barium swallows. In other words, more statistically significant features indicate more different HRCA signals between water and thin liquid barium swallows.

Multiple machine learning classifiers were created and tested to determine if a water or barium swallow can be correctly predicted using HRCA signal features from a random, unlabeled swallow. Three classifiers were tested, including a linear support vector machine (SVM), a Naïve-Bayes classifier, and K-means clustering with 2 clusters. The analyzed data consisted of 36 total features, 9 unique features from the 4 separate signal axes. Each classifier employed principal component analysis (PCA) with 8 principal components. Dimensionality reduction to 8 principal components routinely explained greater than 97% of the variability of the input data.

The total number of swallows is low, so validation is applied. Holdout validation is employed using a train-test split of 70%-30%. The holdout validation strategy is repeated 2,000 times through random initialization of the train and test splits across the dataset each time. The classification accuracies are averaged over all trials to obtain true accuracy measures.

There are multiple measures used to demonstrate the accuracy of each classifier. In medical diagnostic applications, sensitivity (true positives over true positives and false negatives) and specificity (true negatives over true negatives and false positives) are routinely utilized. This study consists of two distinct classes, rather than a direct positive and negative outcome, so distinct accuracy measures are identified in analysis. Overall accuracy (correct classifications over all swallows), barium sensitivity (correct barium classifications over all barium swallows), water sensitivity (correct water classifications over all water swallows), barium predictive value (correct barium classifications over all barium classifications), and water predictive value (correct water classifications over all water classifications). The performance measures employed in this study are illustrated in table 4. All statistical analysis was performed in SAS (SAS Institute, Inc., Cary, North Carolina) and all supervised classifiers were implemented and tested in MATLAB (The MathWorks, Inc, Natick, Massachusetts).

Table 4: Descriptive Measures Employed to Assess Classifier Performance

Classifier Performance Measures		**Actual Material:** Barium	Water	**Predictive Values**
Predicted Material:	Barium	Correct barium classification (A)	Incorrect barium classification (B)	Barium predictive value = $\frac{A}{A+B}$
	Water	Incorrect water classification (C)	Correct Water classification (D)	Water predictive value = $\frac{D}{C+D}$
Sensitivities		Barium sensitivity = $\frac{A}{A+C}$	Water sensitivity = $\frac{D}{B+D}$	Overall accuracy = $\frac{A+D}{A+B+C+D}$

4.0 Results

The feature data used for analysis emanated only from participants with completed swallows using both water and barium. The analyzed data consisted of 185 total swallows, with 90 barium swallows and 95 water swallows from a total of 19 participants. HRCA signals collected for water swallows were significantly longer than barium swallows. Water swallows were roughly segmented by an observer, whereas thin liquid barium swallows were precisely segmented using expert raters and radiographical equipment. Table 5 outlines simple descriptive statistics on the duration and quantity of swallows for each material, while figure 9 illustrates the duration of all barium swallows and all water swallows with matching histograms. Figure 10 illustrates each axis of the raw HRCA signals for a single participant.

Table 5: Relationship Between Quantity, Mean, and Standard Deviation of Length for Barium and Water Swallows

Descriptive Statistic	**Barium**	**Water**
Number of Swallows	90	95
Mean	1.103 seconds	1.468 seconds
Standard Deviation	0.242 seconds	0.375 seconds

The HRCA signals were summarized at the participant level for those with both barium and water swallows. The descriptive statistics for all HRCA signals, including mean and standard deviation, are depicted in table 6.

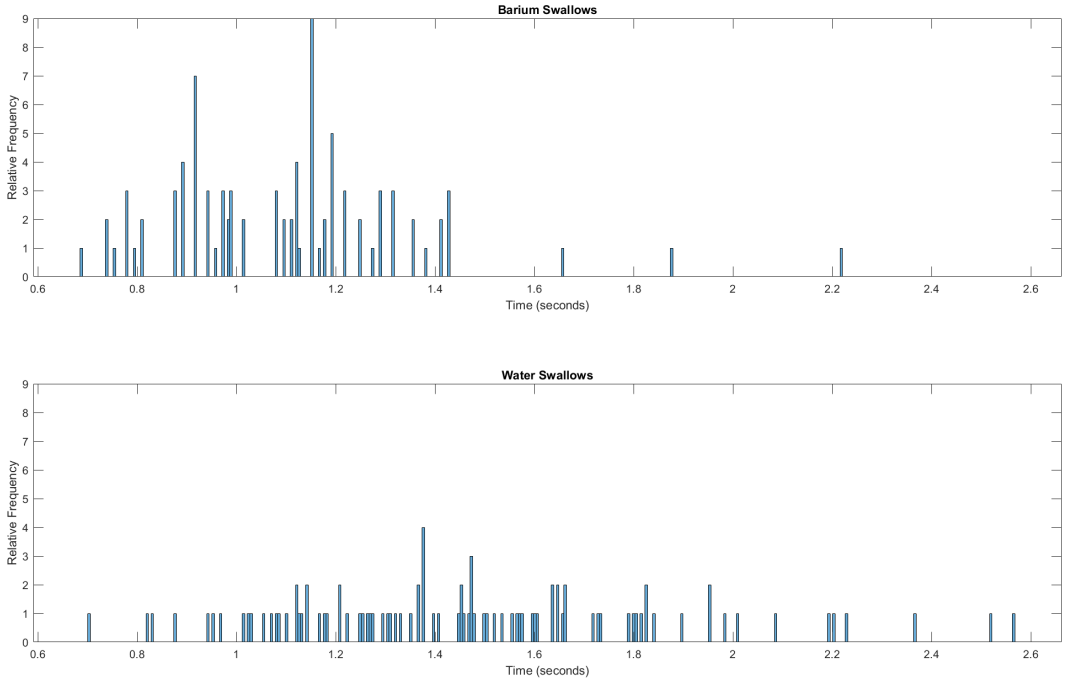

Figure 9: Histogram Comparison of Swallowing Times For Barium Swallows and Water Swallows

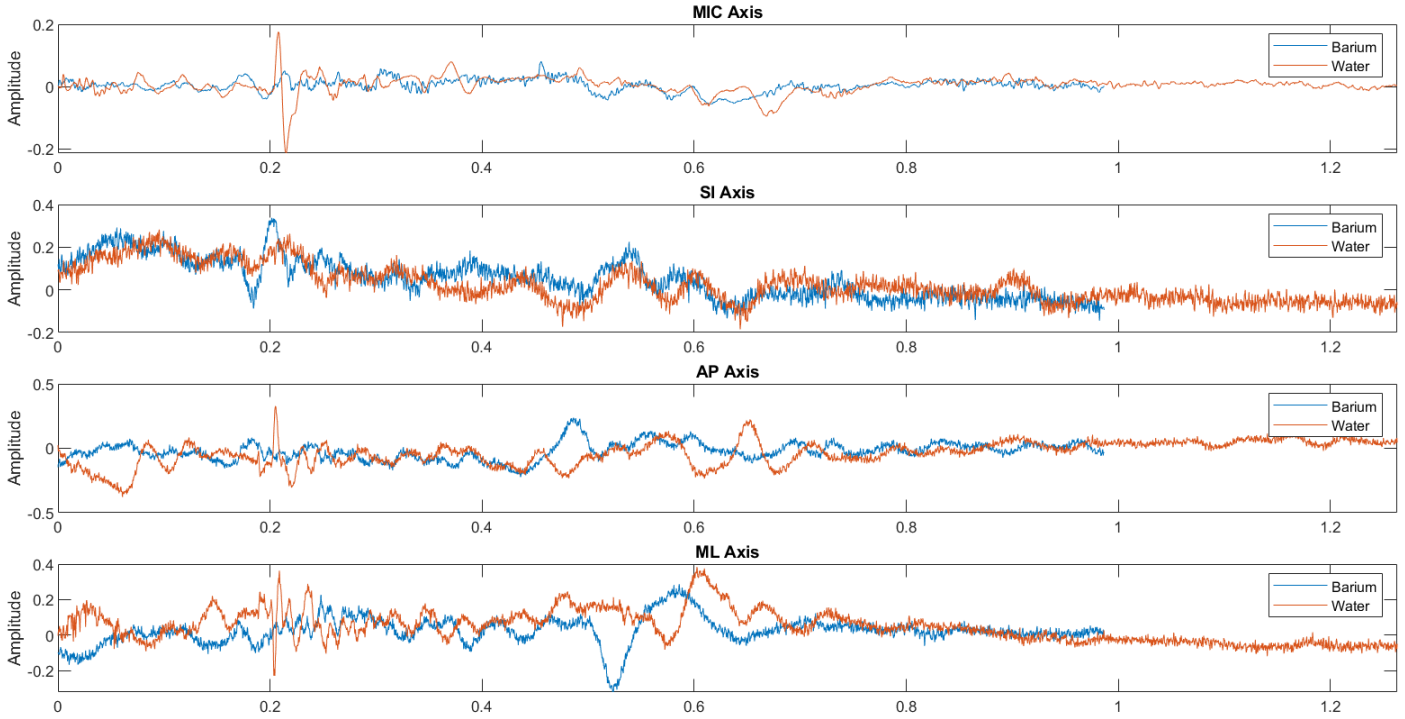

Figure 10: Comparison of Swallowing Sounds and SI, AP, and ML Acceleration Between a Barium Swallow and Water Swallow for a Single Participant

Table 6: Descriptive Statistics (Mean and Standard Deviation) of All HRCA Features For MIC, AP, SS, and ML Axes for Both Barium and Water Swallows

Extracted Features	**MIC**		**AP**		**SI**		**ML**	
Time Domain	Barium	Water	Barium	Water	Barium	Water	Barium	Water
Standard Deviation	0.011 ± 0.014	0.012 ± 0.010	0.010 ± 0.016	0.011 ± 0.015	0.022 ± 0.028	0.024 ± 0.025	0.010 ± 0.011	0.012 ± 0.012
Skewness	-0.543 ± 0.743	-0.825 ± 1.124	-0.185 ± 1.167	-0.002 ± 0.509	-0.140 ± 0.776	-0.029 ± 0.47	0.301 ± 0.831	0.315 ± 0.648
Kurtosis	18.646 ± 17.230	28.804 ± 21.839	13.989 ± 36.581	6.024 ± 13.319	8.274 ± 8.543	8.046 ± 7.883	10.332 ± 16.147	7.936 ± 9.468
Information-Theoretic Domain								
Lempel-Ziv Complexity	0.251 ± 0.057	0.199 ± 0.055	0.224 ± 0.214	0.213 ± 0.199	0.152 ± 0.053	0.145 ± 0.059	0.114 ± 0.031	0.107 ± 0.026
Normalized Entropy Rate	0.909 ± 0.038	0.936 ± 0.022	0.862 ± 0.199	0.891 ± 0.148	0.956 ± 0.010	0.964 ± 0.011	0.961 ± 0.009	0.966 ± 0.009
Frequency Domain								
Peak Frequency (Hz)	9.541 ± 10.085	7.345 ± 8.221	12.741 ± 28.258	0.966 ± 0.409	4.875 ± 4.398	5.118 ± 4.923	2.206 ± 2.671	1.885 ± 1.059
Spectral Centroid (Hz)	63.399 ± 28.587	62.152 ± 28.025	45.395 ± 61.979	25.257 ± 31.512	15.701 ± 18.241	12.667 ± 11.05	35.708 ± 78.885	24.891 ± 39.199
Bandwidth (Hz)	87.298 ± 35.314	86.102 ± 35.349	78.578 ± 69.379	57.405 ± 51.251	33.635 ± 30.592	23.339 ± 15.294	78.019 ± 113.267	57.977 ± 80.418
Time-Frequency Domain								
Wavelet Entropy	1.300 ± 0.478	1.720 ± 0.488	0.211 ± 0.153	0.238 ± 0.16	0.509 ± 0.410	0.842 ± 0.59	0.420 ± 0.459	0.610 ± 0.567

The null hypothesis validated in this study proposes there is no difference between the HRCA signals of a water swallow and a barium swallow. A rejection of the null hypothesis proposes there is a distinct difference in the corresponding HRCA signal feature for a barium and water swallow. The linear mixed models use a confidence level of 0.95 (α=0.05). A p-value less than the significance level of 0.05 indicates a clear rejection of the null hypothesis for the corresponding HRCA signal feature. Table 7 depicts all 36 HRCA signal features with the corresponding p-value sorted from smallest to largest. An HRCA signal feature near the top of table 7 (with a p value ≤ 0.05) indicates a distinct difference for that feature between a barium swallow and water swallow.

The linear mixed models show there is no systematic bias or difference between water and barium swallows for 28 of the 36 HRCA signal features. However, the linear mixed models demonstrate that 8 HRCA signal features exhibit significant difference between water and barium swallows. Table 8 depicts the features that rejected the null hypothesis with the corresponding p-value sorted from smallest to largest. Table 9 depicts the relationship between HRCA axis and the number of rejected features, while table 10 depicts the relationship between the domain of HRCA signals and the number of rejected features.

Table 7: All HRCA Features and Corresponding P-Value

Feature	**P-Value**
MIC Lempel-Ziv Complexity	0.0005
MIC Normalized Entropy Rate	0.0043
MIC Wavelet Entropy	0.0060
MIC Kurtosis	0.0089
SI Wavelet Entropy	0.0146
SI Normalized Entropy Rate	0.0291
ML Standard Deviation	0.0387
AP Normalized Entropy Rate	0.0395
AP Peak Frequency	0.0860
SI Bandwidth	0.1043
ML Wavelet Entropy	0.1146
ML Normalized Entropy Rate	0.1196
AP Spectral Centroid	0.1259
AP Bandwidth	0.1776
MIC Skewness	0.2472
ML Lempel-Ziv Complexity	0.2701
AP Lempel-Ziv Complexity	0.2880
AP Wavelet Entropy	0.3319
MIC Peak Frequency	0.3598
SI Lempel-Ziv Complexity	0.3746
AP Kurtosis	0.3843
SI Spectral Centroid	0.4056
SI Standard Deviation	0.4615
ML Peak Frequency	0.4932
ML Bandwidth	0.5007
ML Kurtosis	0.5073
AP Skewness	0.5388
ML Spectral Centroid	0.5935
SI Skewness	0.6001
AP Standard Deviation	0.6200
MIC Standard Deviation	0.6305
SI Peak Frequency	0.8160
MIC Spectral Centroid	0.8706
SI Kurtosis	0.9138
MIC Bandwidth	0.9152
ML Skewness	0.9493

Table 8: Rejected HRCA Features and Corresponding P-Value

Rejected Feature	**P-Value**
MIC Lempel-Ziv Complexity	0.0005
MIC Normalized Entropy Rate	0.0043
MIC Wavelet Entropy	0.0060
MIC Kurtosis	0.0089
SI Wavelet Entropy	0.0146
SI Normalized Entropy Rate	0.0291
ML Standard Deviation	0.0387
AP Normalized Entropy Rate	0.0395

Table 9: Relationship Between Axis of HRCA Signal and the Number of Rejected Features

Axis of Rejected Feature	**Number of Features**
MIC	4
AP	1
SI	2
ML	1

Table 10: Relationship Between Domain of HRCA Signal and the Number of Rejected Features

Domain of Rejected Feature	**Number of Features**
Time	2
Information-Theoretic	4
Frequency	0
Time-Frequency	2

With or without dimensionality reduction using PCA, none of the classifiers demonstrated high overall accuracy, sensitivity, or predictive values. Dimensionality reduction had no effect on the K-means classifier, marginal effect on the Naïve Bayes classifier, and greatly reduced all performance measures, with the exception of water sensitivity, for the SVM classifier.

Without PCA, the SVM classifier had the highest overall accuracy, while exhibiting similar measures for barium and water sensitivity and predictive value. The Naïve-Bayes and K-means classifiers made correct predictions about half the time. The barium sensitivity for these two classifiers is significantly lower than the water sensitivity. The predictive value for barium and predictive value for water are nearly equal with performance similar to the overall accuracy.

Using PCA for dimensionality reduction, all three classifiers performed similarly. Naïve-Bayes and K-means performed similarly with and without PCA. Each classifier was only able to make a correct prediction around half the time. The barium sensitivity for all three classifiers is significantly lower than the water sensitivity. The predictive value for barium and predictive value for water are nearly equal with performance similar to the overall accuracy.

Table 11 illustrates all five performance measures for all three classifiers without dimensionality reduction, and table 12 illustrates all five performance measures for all three classifiers with dimensionality reduction using principal component analysis.

Table 11: Performance Measures of Classifiers to Detect Swallow Material Using HRCA Signal Features of Barium and Water Swallows Without Dimensionality Reduction

Classifier	**Overall Accuracy**	**Barium Sensitivity**	**Water Sensitivity**	**Barium Predictive Value**	**Water Predictive Value**
SVM	63.186%	61.263%	65.041%	63.125%	63.813%
Naïve Bayes	58.853%	29.519%	87.139%	69.924%	56.267%
K-Means	50.980%	31.252%	70.004%	57.515%	48.989%

Table 12: Performance Measures of Classifiers to Detect Swallow Material Using HRCA Signal Features of Barium and Water Swallows With Dimensionality Reduction Using PCA

Classifier	**Overall Accuracy**	**Barium Sensitivity**	**Water Sensitivity**	**Barium Predictive Value**	**Water Predictive Value**
SVM	52.415%	28.565%	75.414%	54.765%	52.250%
Naïve Bayes	53.371%	24.109%	81.588%	57.284%	52.686%
K-Means	51.078%	30.798%	70.634%	57.444%	49.198%

5.0 Discussion

5.1 Statistical Findings

This study investigated the differences in HRCA signals between thin liquid barium swallows and water swallows through utilizing linear mixed models created for all 36 HRCA signal features. Each linear mixed model operated on the null hypothesis that there is no difference between HRCA signals of a thin liquid barium swallow and a water swallow. The results showed that the null hypothesis is rejected for 8 features. The 8 features with rejected null hypothesis are depicted in table 8, with the frequency of rejected features for each axis and domain represented in table 9 and table 10, respectively. Four of these features emanate from swallowing sounds alone. All the swallows analyzed in this study derive from healthy participants. As healthy swallows ordinarily display no aspiration and minimal noticeable noise, such as choking or coughing, it is expected that amplitude of swallowing sounds will be minimal. Hence, swallowing sounds differing between thin liquid barium swallows and water swallows from a small sample size is conceivable.

As for the domain, 4 (half) of the information-theoretic features and 2 (half) of the time-frequency features had their null hypothesis rejected. These six features account for three quarters of all HRCA features which rejected the null hypothesis. Table 6 illustrates that the Lempel-Ziv complexity is lower, the normalized entropy rate is higher, and the wavelet entropy is higher for all 4 axes of water swallows compared with barium. Lempel-Ziv complexity is a measure of the predictability of a signal [65]. A lower Lempel-Ziv complexity indicates less unique patterns in a finite sequence, thus a less complex signal. Entropy rate realizes the extent of regularity in a signal [62, 57]. A larger value of the normalized entropy rate feature employed in this study demonstrates more regularity in the signal. Wavelet entropy indicates the degree of order in a signal [66]. A higher wavelet entropy demonstrates more disordered signal. The thin liquid barium swallows were segmented by trained professionals using frame-by-frame VFSS. This precise segmentation guarantees the signal duration of a barium swallow contains information from onset to offset of swallow only.

Conversely, water swallows were segmented based on verbal cue and visual observation of the swallowing behavior of the participant. Using a push button integrated in the collection program, a trained operator determined the onset of water swallows when the command of "swallow it" is verbally initiated by the researcher and the offset when the participant is deemed to complete the swallow by visual observation.

Considering the information regarding swallow length for thin liquid barium versus water swallows, it is explainable that these features differ. The HRCA signals from the analyzed water swallows are significantly longer. This information is apparent from table 5 and figure 9. The length of barium swallows is more concentrated around 1 second in length. With water swallows, the lengths appear to be more uniformly distributed between 1 second and 2 seconds. Given the viscosity of water is comparable to the viscosity of Varibar thin, the swallow length (from onset to offset) for each material is presumably equivalent. Thus, the segmented water swallows may contain minimal information before swallow onset and after swallow offset. This extra time with minimal signal information will decrease overall complexity and increase entropy rate given these two features are normalized per signal length, while wavelet entropy will increase given the feature is non-normalized.

5.2 Classifier Findings

Whether or not PCA for dimensionality reduction was employed, the overall accuracy of the classifiers was nearly 50%. With the null hypothesis stating that there is no difference between barium and water swallows, this accuracy metric supports the null hypothesis. However, the barium sensitivity was generally low, and the water sensitivity was high. Given the definition of these two terms illustrated in table 4, a barium swallow was correctly classified infrequently while a water swallow was correctly classified frequently.

To better distinguish the predictability of barium and water swallows, predictive value is an appropriate characteristic. The predictive value is the ratio of correct classifications for a given material to all classifications for the given material. For example, barium predictive value estimates the likelihood that the classified swallow was completed with barium when a

barium swallow was predicted. Barium and water predictive values for the 3 classifiers, with and without dimensionality reduction, are nearly equal around 50%. These performance measures, along with the overall accuracy of the classifiers at approximately 50%, demonstrate an unlabeled set of HRCA signals will essentially be predicted randomly as either performed with barium or water. This metric demonstrates there is no systematic difference between the HRCA signals of a barium swallow and a water swallow.

It is of merit to discuss the performance measures after dimensionality reduction with PCA. In the data set for this study, 8 HRCA signal features exhibit significant differences between a barium swallow and a water swallow. A significant difference between classes (barium and water) in one or more dimensions can cause more separable data. More separable data will make classification accuracy higher. PCA reduces the dimensionality of data by means of projection onto a lower dimensional space. This projection will reduce variability in the data, thereby altering some information contained in the original dataset. The transformation likely emits some information from the 8 rejected features, as these statistically different features exhibit large variability. This claim is demonstrated with the difference in overall accuracy for the SVM and Naïve-Bayes classifiers. Overall accuracy for the SVM classifier drops 10.771% to 52.415% and Naïve-Bayes overall accuracy drops 5.482% to 53.371% after dimensionality reduction with PCA. A SVM machine algorithm creates a linear decision boundary for classification. When variability in the dataset is reduced, each class will appear less linearly separable. Thus, the accuracy decrease for a SVM when PCA is implemented may be due to this reduction of information. The idea of less separable classes may have contributed to the decrease in classification accuracy for the Naïve-Bayes classifier after PCA was utilized. Overall accuracy, along with all other performance measures, is unchanged for the K-means classifier. As K-means clustering involves creation of 2 distinct clusters to classify data, it is understandable that the clusters do not significantly change with PCA. Even with removal of outliers and reduction in class separability, it is unlikely that accuracy of classification will deviate significantly when classification is based on minimum Euclidean distance to cluster centroid.

6.0 Conclusions and Future Work

6.1 Conclusions

This study investigated whether there are statistically significant differences in HRCA signal features between water and thin liquid barium swallows. The purpose of this analysis was part of a preliminary determination as to the feasibility and clinical relevance of using an HRCA based system as a potential method for enhanced bedside swallowing screening and/or an adjunct to clinical swallowing assessment, extending access of screening and diagnostic oropharyngeal dysphagia capabilities to underserved patients. These results indicate no significant difference between HRCA signals of barium and water swallows. Of note, though there is no systematic difference between the HRCA signals of a barium swallow and water swallow, there is insufficient evidence to confirm similarity between the HRCA signals. HRCA signals between both materials do not exhibit differences significant enough to rule out similarity; however, the analyzed data cannot confirm the hypothesis that there is no difference between the HRCA signals of a thin liquid barium swallow and a water swallow. Replication with a larger data set is necessary to sort these remaining questions.

The dataset utilized for analysis and classification consisted of fewer than 100 swallows per material and fewer than 20 participants. Even with utilization of holdout validation for more accurate classification, it is not feasible to conclusively state that these materials are similar, with respect to HRCA signals. The limited observations in the analyzed dataset cannot be used to conclusively confirm similarity.

6.2 Future Work

As a preliminary investigation, this study looked into the similarity or difference of HRCA signals emanating from barium swallows versus water swallows. To further the hypothesis and determine which HRCA signal features exhibit similarity or difference, more data must

be collected and tested to determine if there is a clear correlation between the HRCA signals of a barium swallow and water swallow. Future studies and more data collection will occur to further investigate the findings presented in this study.

Bibliography

[1] P. Clavé and R. Shaker, "Dysphagia: current reality and scope of the problem," *Nature Reviews Gastroenterology and Hepatology*, vol. 12, p. 259, 2015.

[2] D. O. Castell and M. W. Donner, "Evaluation of dysphagia: a careful history is crucial," *Dysphagia*, vol. 2, pp. 65–71, 1987.

[3] C. D. Lind, "Dysphagia: evaluation and treatment," *Gastroenterology Clinics*, vol. 32, pp. 553–575, 2003.

[4] D. A. Lieberman, P. L. D. Garmo, D. E. Fleischer, G. M. Eisen, and M. Helfand, "Patterns of endoscopy use in the united states," *Gastroenterology*, vol. 118, pp. 619–624, 2000.

[5] E. Yazaki, P. Woodland, and D. Sifrim, "Uses of esophageal function testing: dysphagia," *Gastrointestinal Endoscopy Clinics*, vol. 24, pp. 643–654, 2014.

[6] L. Rofes, V. Arreola, J. Almirall, M. Cabré, L. Campins, P. García-Peris, R. Speyer, and P. Clavé, "Diagnosis and management of oropharyngeal dysphagia and its nutritional and respiratory complications in the elderly," *Gastroenterology research and practice*, vol. 2011, 2010.

[7] A. Jean, "Brain stem control of swallowing: neuronal network and cellular mechanisms," *Physiological reviews*, vol. 81, pp. 929–969, 2001.

[8] P. Clavé, M. D. Kraa, V. Arreola, M. Girvent, R. Farre, E. Palomera, and M. Serra-Prat, "The effect of bolus viscosity on swallowing function in neurogenic dysphagia," *Alimentary Pharmacology and Therapeutics*, vol. 24, pp. 1385–1394, 2006.

[9] R. Martino, N. Foley, S. Bhogal, N. Diamant, M. Speechley, and R. Teasell, "Dysphagia after stroke: incidence, diagnosis, and pulmonary complications," *Stroke*, vol. 36, pp. 2756–2763, 2005.

[10] M. Aslam and M. F. Vaezi, "Dysphagia in the elderly," *Gastroenterology and Hepatology*, vol. 9, p. 784, 2013.

[11] M. Serra-Prat, G. Hinojosa, D. López, M. Juan, E. Fabré, D. S. Voss, M. Calvo, V. Marta, L. Ribó, E. Palomera, *et al.*, "Prevalence of oropharyngeal dysphagia and impaired safety and efficacy of swallow in independently living older persons," *Journal of the American Geriatrics Society*, vol. 59, pp. 186–187, 2011.

[12] I. J. Cook, "Oropharyngeal dysphagia," *Gastroenterology Clinics*, vol. 38, pp. 411–431, 2009.

[13] M. R. Spieker, "Evaluating dysphagia," *American Family Physician*, vol. 61, pp. 3639–3648, 2000.

[14] I. A. Humbert and J. Robbins, "Dysphagia in the elderly," *Physical Medicine and Rehabilitation Clinics of North America*, vol. 19, pp. 853–866, 2008.

[15] E. S. Eisenstadt, "Dysphagia and aspiration pneumonia in older adults," *Journal of the American Academy of Nurse Practitioners*, vol. 22, pp. 17–22, 2010.

[16] L. A. Mandell and M. S. Niederman, "Aspiration pneumonia," *New England Journal of Medicine*, vol. 380, pp. 651–663, 2019.

[17] J. C. Rosenbek, J. A. Robbins, E. B. Roecker, J. L. Coyle, and J. L. Wood, "A penetration-aspiration scale," *Dysphagia*, vol. 11, pp. 93–98, 1996.

[18] T. Manzoor, Z. Suman, M. Ibrahim, R. Azmat, and S. Tahira, *Effectiveness of Swallowing Exercises in Dysphagia: A Speech-Pathologist Perspective*. PhD thesis, 2015.

[19] M. Saconato, B. M. Chiari, H. M. Lederman, and M. I. R. Gonçalves, "Effectiveness of chin-tuck maneuver to facilitate swallowing in neurologic dysphagia," *International Archives of Otorhinolaryngology*, vol. 20, pp. 13–17, 2016.

[20] P. Clavé, M. D. Kraa, V. Arreola, M. Girvent, R. Farre, E. Palomera, and M. Serra-Prat, "The effect of bolus viscosity on swallowing function in neurogenic dysphagia," *Alimentary Pharmacology and Therapeutics*, vol. 24, pp. 1385–1394, 2006.

[21] A. J. Miller, "The neurobiology of swallowing and dysphagia," *Developmental Disabilities Research Reviews*, vol. 14, pp. 77–86, 2008.

[22] K. Matsuo and J. B. Palmer, "Anatomy and physiology of feeding and swallowing: normal and abnormal," *Physical Medicine and Rehabilitation Clinics of North America*, vol. 19, pp. 691–707, 2008.

[23] A. J. Miller, "Neurophysiological basis of swallowing," *Dysphagia*, vol. 1, p. 91, 1986.

[24] N. Lucci, C. McConnell, and C. Biddle, "Understanding normal and abnormal swallowing: Patient safety considerations for the perianesthetic nurse," *Journal of Peri-Anesthesia Nursing*, vol. 33, pp. 375–388, 2018.

[25] C. A. S. Hammond and L. B. Goldstein, "Cough and aspiration of food and liquids due to oral-pharyngeal dysphagia: Accp evidence-based clinical practice guidelines," *Chest*, vol. 129, p. 154S–168S, 2006.

[26] C. V. Hughes, B. J. Baum, P. C. Fox, Y. Marmary, C.-K. Yeh, and B. C. Sonies, "Oral-pharyngeal dysphagia: a common sequela of salivary gland dysfunction," *Dysphagia*, vol. 1, pp. 173–177, 1987.

[27] S. M. Shaw and R. Martino, "The normal swallow: muscular and neurophysiological control.," *Otolaryngologic Clinics of North America*, vol. 46, pp. 937–956, 2013.

[28] R. M. noz, L. Ibáñez, J. Salinas, A. Escalona, G. Pérez, F. Pimentel, S. Guzmán, and C. Boza, "Importance of routine preoperative upper gi endoscopy: why all patients should be evaluated?," *Obesity Surgery*, vol. 19, pp. 427–431, 2009.

[29] R. Yadlapati, "High-resolution esophageal manometry: interpretation in clinical practice," *Current Opinion in Gastroenterology*, vol. 33, p. 301, 2017.

[30] D. C. Sadowski and L. Broenink, "High-resolution esophageal manometry: a time motion study," *Canadian Journal of Gastroenterology*, vol. 22, 2008.

[31] E. Sejdić, G. A. Malandraki, and J. L. Coyle, "Computational deglutition: Using signal-and image-processing methods to understand swallowing and associated disorders [life sciences]," *IEEE Signal Processing Magazine*, vol. 36, pp. 138–146, 2018.

[32] S. G. Hiss and G. N. Postma, "Fiberoptic endoscopic evaluation of swallowing," *The Laryngoscope*, vol. 113, pp. 1386–1393, 2003.

[33] J. W. Lee, D. R. Randall, L. M. Evangelista, M. A. Kuhn, and P. C. Belafsky, "Subjective assessment of videofluoroscopic swallow studies," *Otolaryngology–Head and Neck Surgery*, vol. 156, pp. 901–905, 2017.

[34] B. Martin-Harris and B. Jones, "The videofluorographic swallowing study," *Physical Medicine and Rehabilitation Clinics of North America*, vol. 19, pp. 769–785, 2008.

[35] J. A. Y. Cichero and B. E. Murdoch, "Acoustic signature of the normal swallow: characterization by age, gender, and bolus volume," *Annals of Otology, Rhinology and Laryngology*, vol. 111, pp. 623–632, 2002.

[36] C. Borr, M. Hielscher-Fastabend, and A. Lücking, "Reliability and validity of cervical auscultation," *Dysphagia*, vol. 22, pp. 225–234, 2007.

[37] C. Yu, Y. Khalifa, and E. Sejdić, "Silent aspiration detection in high resolution cervical auscultations," in *2019 IEEE EMBS International Conference on Biomedical and Health Informatics (BHI)*, pp. 1–4, 2019.

[38] J. L. Coyle and E. Sejdić, "High-resolution cervical auscultation and data science: new tools to address an old problem," *American Journal of Speech-Language Pathology*, vol. 29, pp. 992–1000, 2020.

[39] F. Movahedi, A. Kurosu, J. L. Coyle, S. Perera, and E. Sejdić, "A comparison between swallowing sounds and vibrations in patients with dysphagia," *Computer Methods and Programs in Biomedicine*, vol. 144, pp. 179–187, 2017.

[40] J. M. Dudik, J. L. Coyle, A. El-Jaroudi, Z.-H. Mao, M. Sun, and E. Sejdić, "Deep learning for classification of normal swallows in adults," *Neurocomputing*, vol. 285, pp. 1–9, 2018.

[41] S. Mao, Z. Zhang, Y. Khalifa, C. Donohue, J. L. Coyle, and E. Sejdić, "Neck sensor-supported hyoid bone movement tracking during swallowing," *Royal Society Open Science*, vol. 6, p. 181982, 2019.

[42] Y. Khalifa, J. L. Coyle, and E. Sejdić, "Non-invasive identification of swallows via deep learning in high resolution cervical auscultation recordings," *Scientific Reports*, vol. 10, pp. 1–13, 2020.

[43] S. Mao, A. Sabry, Y. Khalifa, J. L. Coyle, and E. Sejdić, "Estimation of laryngeal closure duration during swallowing without invasive x-rays," *Future Generation Computer Systems*, vol. 115, pp. 610–618, 2020.

[44] R. Martino, F. Silver, R. Teasell, M. Bayley, G. Nicholson, D. L. Streiner, and N. E. Diamant, "The toronto bedside swallowing screening test (tor-bsst) development and validation of a dysphagia screening tool for patients with stroke," *Stroke*, vol. 40, pp. 555–561, 2009.

[45] D. M. Suiter and S. B. Leder, "Clinical utility of the 3-ounce water swallow test," *Dysphagia*, vol. 23, pp. 244–250, 2008.

[46] H. L. Warner, D. M. Suiter, K. V. Nystrom, K. Poskus, and S. B. Leder, "Comparing accuracy of the yale swallow protocol when administered by registered nurses and speech-language pathologists," *Journal of Clinical Nursing*, vol. 23, pp. 1908–1915, 2014.

[47] M. González-Fernández, M. T. Sein, and J. B. Palmer, "Clinical experience using the mann assessment of swallowing ability for identification of patients at risk for aspiration in a mixed-disease population," *American Journal of Speech-Language Pathology*, 2011.

[48] N. Antonios, G. Carnaby-Mann, M. Crary, L. Miller, H. Hubbard, K. Hood, R. Sambandam, A. Xavier, and S. Silliman, "Analysis of a physician tool for evaluating dysphagia on an inpatient stroke unit: the modified mann assessment of swallowing ability," *Journal of Stroke and Cerebrovascular Diseases*, vol. 19, pp. 49–57, 2010.

[49] W. W. Stroup, *Generalized linear mixed models: modern concepts, methods and applications*. Boca Raton, FL, London, UK, New York, NY: CRC Press/Taylor and Francis, 2012.

[50] C. M. Bishop, *Pattern Recognition and Machine Learning (Information Science and Statistics)*. Berlin, Heidelberg: Springer-Verlag, 2006.

[51] A. Leon-Garcia, *Probability, Statistics, and Random Processes for Electrical Engineering*. Upper Saddle River, NJ: Pearson/Prentice Hall, third ed., 2008.

[52] C. M. Steele, "Mapping bracco's varibar® barium products to the iddsi framework," 2017. Accessed Nov. 23 2020.

[53] J. M. Dudik, A. Kurosu, J. L. Coyle, and E. Sejdić, "A statistical analysis of cervical auscultation signals from adults with unsafe airway protection," *Journal of Neuroengineering and Rehabilitation*, vol. 13, p. 7, 2016.

[54] K. Takahashi, M. E. Groher, and K. ichi Michi, "Methodology for detecting swallowing sounds," *Dysphagia*, vol. 9, pp. 54–62, 1994.

[55] Y. Khalifa, C. Donohue, J. L. Coyle, and E. Sejdić, "Upper esophageal sphincter opening segmentation with convolutional recurrent neural networks in high resolution cervical auscultation," *IEEE Journal of Biomedical and Health Informatics*, 2020.

[56] J. Lee, C. M. Steele, and T. Chau, "Time and time–frequency characterization of dual-axis swallowing accelerometry signals," *Physiological Measurement*, vol. 29, p. 1105, 2008.

[57] E. Sejdić, V. Komisar, C. M. Steele, and T. Chau, "Baseline characteristics of dual-axis cervical accelerometry signals," *Annals of Biomedical Engineering*, vol. 38, pp. 1048–1059, 2010.

[58] E. Sejdić, C. M. Steele, and T. Chau, "The effects of head movement on dual-axis cervical accelerometry signals," *BMC Research Notes*, vol. 3, pp. 1–6, 2010.

[59] E. Sejdić, C. M. Steele, and T. Chau, "A method for removal of low frequency components associated with head movements from dual-axis swallowing accelerometry signals," *PLoS One*, vol. 7, p. e33464, 2012.

[60] E. Sejdić, C. M. Steele, and T. Chau, "A procedure for denoising dual-axis swallowing accelerometry signals," *Physiological Measurement*, vol. 31, p. N1, 2009.

[61] C. Donohue, Y. Khalifa, S. Perera, E. Sejdić, and J. L. Coyle, "A preliminary investigation of whether hrca signals can differentiate between swallows from healthy people and swallows from people with neurodegenerative diseases," *Dysphagia*, pp. 1–9, 2020.

[62] J. Lee, E. Sejdić, C. M. Steele, and T. Chau, "Effects of liquid stimuli on dual-axis swallowing accelerometry signals in a healthy population," *BioMedical Engineering OnLine*, vol. 9, p. 7, 2010.

[63] C. Donohue, Y. Khalifa, S. Perera, E. Sejdić, and J. L. Coyle, "How closely do machine ratings of duration of ues opening during videofluoroscopy approximate clinician

ratings using temporal kinematic analyses and the mbsimp?," *Dysphagia*, pp. 1–12, 2020.

[64] C. Donohue, S. Mao, E. Sejdić, and J. L. Coyle, "Tracking hyoid bone displacement during swallowing without videofluoroscopy using machine learning of vibratory signals," *Dysphagia*, pp. 1–11, 2020.

[65] M. Aboy, R. Hornero, D. Abásolo, and D. Álvarez, "Interpretation of the lempel-ziv complexity measure in the context of biomedical signal analysis," *IEEE transactions on Biomedical Engineering*, vol. 53, pp. 2282–2288, 2006.

[66] O. A. Rosso, S. Blanco, J. Yordanova, V. Kolev, A. Figliola, M. Schürmann, and E. Başar, "Wavelet entropy: a new tool for analysis of short duration brain electrical signals," *Journal of Neuroscience Methods*, vol. 105, pp. 65–75, 2001.